cmgh
CELLULAR AND MOLECULAR GASTROENTEROLOGY AND HEPATOLOGY

ORIGINAL RESEARCH

siRNA Library Screening Identifies a Druggable Immune-Signature Driving Esophageal Adenocarcinoma Cell Growth

Shane P. Duggan,[1,2,3] Catherine Garry,[4] Fiona M. Behan,[4] Sinead Phipps,[4] Hiromi Kudo,[5] Murat Kirca,[4,6] Abdul Zaheer,[6] Sarah McGarrigle,[7] John V. Reynolds,[7] Robert Goldin,[5] Steve E. Kalloger,[8] David F. Schaeffer,[8] Aideen Long,[4] Jessica Strid,[3] and Dermot Kelleher[1,2,4]

[1]Department of Medicine, Division of Gastroenterology, [2]Life Science Institute, [8]Department of Pathology and Laboratory Medicine, University of British Columbia, Vancouver, British Columbia, Canada; [3]Centre for Complement and Inflammation Research, [5]Centre for Pathology, St Mary's Hospital, Imperial College London, London, United Kingdom; [4]Department of Clinical Medicine, [7]Department of Surgery, Trinity Translational Medicine Institute, Trinity College Dublin, Dublin, Ireland; [6]Department of Gastroenterology, St James' Hospital, Dublin, Ireland

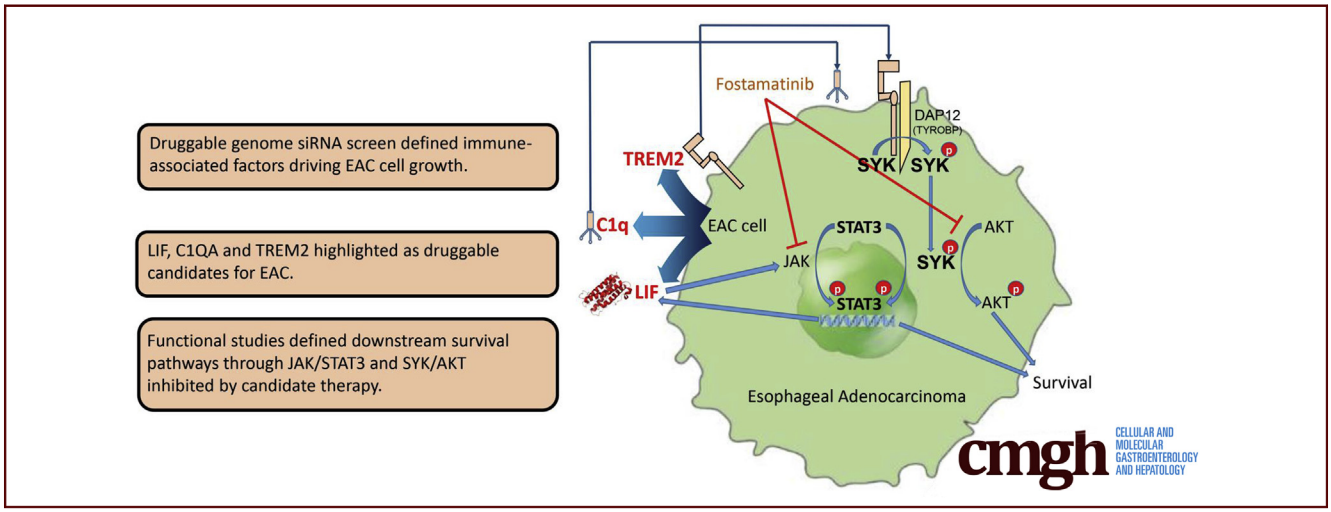

SUMMARY

This study defines immune-associated factors supportive of esophageal adenocarcinoma cell growth through small interfering RNA screening and pathologic and functional studies. Fostamatinib R788, targeting Janus kinase/signal transducer-and-activator of transcription and TYRO protein tyrosine kinase binding protein/spleen tyrosine kinase/AKT serine-threonine kinase pathways, induced esophageal adenocarcinoma cell death and reduced tumor burden in xenografted mice.

BACKGROUND & AIMS: Effective therapeutic approaches are urgently required to tackle the alarmingly poor survival outcomes in esophageal adenocarcinoma (EAC) patients. EAC originates from within the intestinal-type metaplasia, Barrett's esophagus, a condition arising on a background of gastroesophageal reflux disease and associated inflammation.

METHODS: This study used a druggable genome small interfering RNA (siRNA) screening library of 6022 siRNAs in conjunction with bioinformatics platforms, genomic studies of EAC tissues, somatic variation data of EAC from The Cancer Genome Atlas data of EAC, and pathologic and functional studies to define novel EAC-associated, and targetable, immune factors.

RESULTS: By using a druggable genome library we defined genes that sustain EAC cell growth, which included an unexpected immunologic signature. Integrating Cancer Genome Atlas data with druggable siRNA targets showed a striking concordance and an EAC-specific gene amplification event associated with 7 druggable targets co-encoded at Chr6p21.1. Over-representation of immune pathway–associated genes supporting EAC cell growth included leukemia inhibitory factor, complement component 1, q subcomponent A chain (C1QA), and triggering receptor expressed on myeloid cells 2 (TREM2), which were validated further as targets sharing downstream signaling pathways through genomic and pathologic studies. Finally, targeting the triggering receptor expressed on myeloid cells 2-, C1q-, and leukemia inhibitory factor–activated signaling pathways (TYROBP–spleen tyrosine kinase and JAK-STAT3) with spleen tyrosine kinase and Janus-activated kinase inhibitor fostamatinib R788 triggered EAC cell death, growth arrest, and reduced tumor burden in NOD scid gamma mice.

CONCLUSIONS: These data highlight a subset of genes co-identified through siRNA targeting and genomic studies of expression and somatic variation, specifically highlighting the contribution that immune-related factors play in support of EAC development and suggesting their suitability as targets in the treatment of EAC. *(Cell Mol Gastroenterol Hepatol 2018;5:569–590; https://doi.org/10.1016/j.jcmgh.2018.01.012)*

Keywords: Esophageal Adenocarcinoma; Barrett's Esophagus; Inflammation; Therapeutic Targets.

See editorial on page 652.

The rates of esophageal adenocarcinoma (EAC) have increased steadily over the past number of decades at an average of 2.8% per year in the most recent North American data.[1,2] Comparatively, the incidence rates of more prevalent cancers such as lung, prostate, colon, and breast cancer have seen marginal decreases in recent years.[2] Current curative approaches for EAC typically involve surgical esophagectomy or endoscopic resection in early T1 cancers, or chemotherapy plus esophagectomy in which limited invasion has occurred. The survival rate for EAC is 18% at 5 years compared with 90% and 91% for breast and colon, respectively.[2] Therefore, preventative and targeted therapies for EAC are urgently needed to increase survival rates and reduce tumor burden.

Targeted therapeutics for EAC have been hindered by the heterogeneous nature of patient-specific somatic mutations and copy number variations, the differing spectrum of mutations between patients and a poorly defined map of the molecular drivers of this cancer type. The most prevalent mutations or copy number variations have been reported in presently nonactionable tumor-suppressor genes such as *TP53, ELMO1, CDKN2A, SMAD4,* and *ARID1A,* rather than driver oncogenes,[3–10] and also prominently are observed in the precancerous metaplastic tissues of EAC and non-EAC patients.[4,11] Common amplifications have been reported in *KRAS* (21%), *ERBB2/HER2* (19%), and *EGFR* (16%), and deletions in *SMAD4* and *CDKN2A*. Targeted therapies based on these amplifications and mutations have largely been ineffective, except in the case of HER-2–positive gastric and junctional tumors, in which trastuzumab improved outcomes in metastatic patients.[12–14] Therefore, further cellular targets independent of, or harmonizing with, the mutational status of EAC are warranted to expand the repertoire of potential targeted therapeutic approaches.

The development of EAC is believed to progress from within the metaplastic lesion, Barrett's esophagus (BE), supported by chronic inflammatory gastroesophageal reflux disease (GERD) in which chronic reflux of gastric and bile acids into the esophagus induces epithelial inflammation, ulceration, and epithelial erosion.[15,16] However, cytokine-mediated structural alterations within the esophageal epithelium may also arise without the need for reflux-mediated epithelial erosion.[17] Our laboratory and others have shown that esophageal epithelial cells release proinflammatory cytokines such as interleukin (IL)6, IL8, and IL1β in response to acid and bile acids that may become overexpressed in EAC partially as a result of reduced tribbles pseudokinase 3 (TRIB3) expression.[18–24] These cytokines result in greater numbers of immune cells infiltrating the epithelium where they initially are associated with basal cell and papillary hyperplasia without loss of surface cells.[17] However, the mechanistic links between this inflammatory milieu, the metaplastic process, and EAC cell growth or oncogenesis is poorly detailed and has yet to result in actionable targets for therapeutic intervention in patients presenting with EAC. Thus, our understanding of inflammatory or immune-mediated promotion of EAC is incomplete and requires further exploration to both treat and prevent this deadly disease. Herein, using functional genomic screens we show a distinct targetable EAC-specific immune-pathway–associated signature driving sustained oncogenic growth.

Materials and Methods

Cell Lines and Cell Culture

FLO-1 (11012001), SK-GT-4 (11012007), and OE33 (96070808) cell lines were obtained from The European Collection of Authenticated Cell Cultures (ECACC). CP-D (CP-18821) cell lines were obtained from the American Type Culture Collection (ATCC). Validation of findings was performed in multiple esophageal EAC cell lines (SKGT4, FLO-1, and OE-33), which have been obtained from commercial sources and tested by STR profiling. CP-D cells were cultured in bronchial epithelial base/growth media (Lonza, Mississauga, Canada) with bullet kit additives and 5% fetal bovine serum (Gibco, Invitrogen, Carlsbad, CA). SKGT4, OE-33, and FLO-1 cells were maintained in RPMI1640 without L-glutamine media with 10% fetal bovine serum (Gibco, Invitrogen) and added penicillin/streptomycin/L-glutamine (Gibco). Cells were fed at 48 hours, and subcultured at 72 hours, before overconfluence, using trypsin-EDTA (Gibco) in Hank's balanced salt solution for detachment. Treatments with recombinant leukemia inhibitory factor (LIF) (30 ng/mL, ab57665; Abcam), IL6 (30 ng/mL; R&D Systems, Minneapolis, MN), native C1q (75 μg/mL; Sigma, Oakville, Ontario), and IL6 blocking antibody (AB206NA) experiments were performed in either 6- or 96-well cell culture plates for protein and viability experiments, respectively.

Abbreviations used in this paper: **ATCC, American Type Culture Collection; BE, Barrett's esophagus; EAC, esophageal adenocarcinoma; ERBB2, erb-b2 receptor tyrosine kinase 2; ESCC, esophageal squamous cell carcinoma; FCS, fetal calf serum; GEM, gene expression microarray; GERD, gastroesophageal reflux disease; GO, gene ontology; HGD, high-grade dysplastic; IL, interleukin; LIF, leukemia inhibitory factor; JAK-STAT, Janus kinase/signal transducer-and-activator of transcription; mRNA, messenger RNA; MTT, 3-(4,5-dimethylthiazol-2-yl)-2,5-diphenyltetrazolium bromide; PBS, phosphate-buffered saline; RA, rheumatoid arthritis; siRNA, small interfering RNA; SV, somatic variation; SYK, spleen tyrosine kinase; TCGA, The Cancer Genome Atlas; TREM2, triggering receptor expressed on myeloid cells 2; VEGFA, vascular endothelial growth factor A.**

Most current article

2352-345X
https://doi.org/10.1016/j.jcmgh.2018.01.012

Clinical Tissue Collection, RNA Extraction, and Immunohistochemistry

Sample size for messenger RNA (mRNA) expression analysis of immune-related factors in BE (N = 17) and EAC (N = 23) patients and controls (N = 17) was determined through previous use of this clinical cohort in published reports.[25] Written, oral, and informed consent was provided by all patients who contributed tissue biopsy specimens for gene expression aspects of this study. Ethical approval for this study was granted by the Research Ethics Committee of Tallaght Hospital and St. James' Hospital (Dublin, Ireland) and performed in accordance with the associated guidelines. The sample size for immune-histopathologic staining was determined by tissue availability and from previous use of BE cohorts (n = 28) and was scored by 2 independent pathologists. The retrospective cohort was processed with a Leica BOND-MAX automated immunohistochemistry processing unit (Leica, Concord, Ontario, Canada) using primary antibodies to C1QA (ab76425; Abcam, Cambridge, United Kingdom) and triggering receptor expressed on myeloid cells 2 (TREM2) (HPA012571; Sigma) at a concentration of 1:50 and 1:100, respectively. Institutional ethics approval was obtained for the use of EAC and control tissue from the University of British Columbia research ethics board (H17-01285). Slides were scanned with an Aperio slide scanner (Leica) and digitally magnified images were produced in ImageScope (Leica).

Small Interfering RNA–Mediated Silencing

Small interfering RNA (siRNA) smart pools, siGenome-SMARTpool (Thermo Fischer) for initial screening, or siON-TARGETplus (Thermo Fischer) in all other validation experiments were delivered to cells using Dharmafect transfection reagent (DF1-4; (Thermo Fischer)) using a reverse transfection protocol. Transfection reagent:siRNA complexes were added, as per the manufacturer's instructions, to seeded but unattached cells in culture media (BEGM or RPMI) without fetal calf serum (FCS) or penicillin/streptomycin/L-glutamine, and allowed to incubate for 24 hours before replacement of the media with media containing FCS for 72 hours before analysis. Experiments performed in 6-, 24-, and 96-well cell culture plates were seeded with 2×10^5, 5×10^4, and 3×10^3 cells, respectively, in reverse transfection protocols. This method used siRNA (25 nmol/L) combined with 0.2 μL Dharmafect transfection reagent (Thermo Fischer).

High-Throughput siRNA Library Screening

The objectives of this study were to define therapeutically targetable regulators of esophageal cancer growth and survival. The initial siRNA library screen was performed in CP-D cells (n = 8 with replicate plate discarded, plates 2–4 used for 3-(4,5-dimethylthiazol-2-yl)-2,5-diphenyltetrazolium bromide [MTT] assays). The human druggable siRNA library consisting of 6022 siRNA pools (4 individual gene targeting siRNAs at 20 μmol/L) formatted in 76 library plates (96-well v bottom) was maintained and re-aliquoted into a v bottom 96-well daughter library plate (Thermo Fischer) containing siBuffer (Thermo Fischer) to a concentration of 5 μmol/L using a plate replicator within a biosafety cabinet (Matrix/Thermo Fischer). Each daughter plate provides enough siRNA for 8 assay plates at 25 nmol/L. Negative (nontargeting siRNA pool) and positive controls (siRNA pool targeting GATA6), 25 nmol/L each, were added to columns 1 and 2 of 96-well v bottom plates. Reverse siRNA transfection plates then were prepared from these daughter plates through the distribution of transfection cocktail (1:100 μL DF4 in culture media) throughout all 76 transfection plates using electronic multichannel pipette delivery. Each transfection plate was individually mixed by swirling and tapping after completion and then was incubated for 20 minutes before distribution into assay plates sequentially (n = 8 replicate plates, 20 μL per well). An automated multichannel dispenser (Wellmate, Thermo Fischer, Waltham, MA) was next used to distribute 80 μL culture media per well containing 5×10^3 cells to create the assay plates. Cell culture media was replaced at 24 hours with full media containing FCS and incubated for a further 72 hours before the addition of 10 μL MTT reagent at 93 hours and dimethyl sulfoxide containing detergent reagent at 96 hours after a 3-hour incubation at 37°C. Plates were allowed to incubate at room temperature in the dark overnight before measuring absorbance at 570 nm. Screening results were analyzed in R statistical software using CellHTS2[26,27] (https://bioconductor.org) and RNAither[28] (https://bioconductor.org) platform for statistical analysis of high-throughput RNA interference screens. The median of negative controls was used for within-plate normalization and furthermore to perform interplate normalization of replicate plates. The screening Z-factor was calculated as follows:

$$Z = 1 - \frac{[3(\text{SDsample}) + 3(\text{SDcontrol})]}{|\text{mean sample} - \text{mean control}|}$$

Screening results were ranked by robust Z score as calculated in RNAither with a cut-off value of -1.645 and a cell viability score less than 50%. Outliers were only removed with clear justification, such as an infection in a replicate well. Bioinformatic interpretation of siRNA screening results linked significant regulators of CP-D cell growth with immune-related pathways using n = 3 informatic platforms. Gene ontology–enrichment analysis was performed using Fatigo in Babelomics 5.0 (http://babelomics.bioinfo.cipf.es/) with identification list vs background reference druggable genome reference gene list and ClueGO gene ontology networking with Cytoscape plugin (http://apps.cytoscape.org/apps/cluego).

Protein Expression Analysis

Samples for protein expression analysis by Western blot were collected from 6-well plates at 72 hours for validation of siRNA-mediated silencing effects by scraping in ice-cold phosphate-buffered saline (PBS). The cells were then pelleted by centrifugation before resuspension in M-PER lysis solution (Pierce, Thermo Fischer) and incubation on ice for 10 minutes as per the manufacturer's instructions. Protein concentration was determined by

micro–bicinchoninic acid assay at 562 nm (Pierce, Thermo Fischer) to allow equal loading of protein in sodium dodecyl sulfate–polyacrylamide (SDS-PAGE) gel electrophoresis. Proteins separated by SDS-PAGE were transferred to a polyvinylidene difluoride membrane in semidry conditions in a power blotter (Pierce, Thermo Fischer) as previously described.[18,19,22,25] Membranes were collected in PBS followed by incubation in milk protein–based blocking solution for 30 minutes. Primary antibodies to LIF, C1QA (ab108325; Abcam), TREM2 (Sigma), TYROBP or DAP12 (ab124834; Abcam), spleen tyrosine kinase (SYK) (D3Z1E; Cell Signaling), and p-SYK (Cell Signaling) were diluted in blocking solution at 1:1000, 1:500, 1:250, 1:300, 1:300, and 1:200, respectively, and incubated with the appropriate membranes for 24 hours at 4°C followed by washing with PBS-Tween and further room temperature incubation with appropriate secondary horseradish-peroxidase–conjugated antibody at a 1:2000 dilution for 2 hours. Chemiluminescent signals were detected using both radiograph film (TREM2, DAP12, SYK, p-SYK, C1QA and Actin) and cooled LCD camera lightbox (LIF, pSTAT3, and Actin) (Bio-Rad).

Gene Expression Microarray Re-analysis and Bioinformatics

Data sets derived from Kim et al,[29] Kimchi et al,[30] and Ostrowski et al[31] were re-analyzed in Genespring GX (Agilent, Santa Clara, CA) as described previously.[25] The expression of genes whose siRNA-mediated silencing resulted in greater than 50% cell death and a Z score level $<$-1.645 were examined in the gene expression microarray (GEM) data sets of BE and EAC tissues. These GEM studies were analyzed at a Mann–Whitney significance level of $P <$ .001. Results were hierarchically clustered by genes and samples using Euclidean distance and viewed through the data set of Kim et al[29] for ease of representation.

Cellular Assays of Viability, Apoptosis, and Gene Expression

Measurements of cell viability were performed after transfection of cells with the siRNA and/or treatment with recombinant or native proteins using the MTT assay (LONZA, Mississauga, Canada). Briefly, when recombinant (LIF and IL6) or native proteins (C1q and anti-IL6) were used, at the listed concentrations, these were added at 72 hours after transfection with siRNA followed by end point assays of viability (N = 3) or gene expression (N = 3) at 96 hours. In viability assays using siRNA-mediated gene inhibition, 10 μL of MTT reagent (30-1010K; ATCC) was added to each well 93 hours after transfection using a multichannel repetman (Thermo Scientific), and then incubated for 3 hours at 37°C. Detergent reagent (100 μL, 30-1010K; ATCC) was then added using a multichannel repetman (Rainin, Mississauga, Canada). Plates then were covered with tin foil to protect them from light and left at room temperature overnight. Cell viability was calculated by reading the absorbance at 570 nm using a spectrophotometer (Tecan Spark 10 M, Männedorf, Switzerland). In experiments using fostamatinib R406, cells were treated with R406 or vehicle dimethyl sulfoxide at the listed concentration for 24 hours followed be measurement of cell viability. Cellular growth arrest and apoptosis after R406 treatment was determined through flow-cytometric cell-cycle analysis using fluorescein isothiocyanate–labeled bromodeoxyuridine incorporation and a 7-AAD staining kit (BD Biosciences, San Jose, CA), as per the manufacturer's instructions, and analyzed using a BD FACSVerse (BD Biosciences, San Jose, CA). Cells undergoing growth arrest were defined by a decreased percentage of cells in the S phase (R4) and a gain of those in G0/G1 (R3). Cells undergoing apoptosis were defined by a decreased percentage of cells in the S phase and a gain in both G0/G1 (R3) and sub-G1 populations (R6). Controls including deoxycholate treatment (200 μmol/L) and cells in culture media lacking FCS (resting-FCS) were used to define cell populations in apoptosis and growth arrest, respectively.

Gene Expression Analysis

As outlined in previous publications,[18,25] gene expression analysis was performed by real-time relative reverse-transcription polymerase chain reaction using a 7900HT thermocycler with predesigned real-time primers and probes (Applied Biosystems, Foster City, CA). Relative fold changes in mRNA expression levels were calculated using the delta delta Ct method and glyceraldehyde-3-phosphate dehydrogenase as the denominator control gene. Mean values from control resting, nontargeting siRNA–transfected cells or esophageal squamous tissues were used as a base level from which to calculate altered expression. Nonparametric Mann–Whitney testing appropriate for real-time reverse-transcription polymerase chain reaction data was used to examine the significance of the observed changes.

Murine Subcutaneous Xenografts

Animal studies were conducted in accordance with the Imperial College Animal Welfare and Ethical Review Body of the UK Home Office for Laboratory Animal Care regulations following the Animal Research: Reporting In Vivo Experiments guidelines.[32] Six-week-old female NOD/SCIDgamma mice were obtained from Harlan Laboratories (Cambridge, UK) and maintained in individually vented cages at 5 animals per cage and water and food were provided ad libitum, as per institutional guidelines. At t0, 1×10^6 OE-33 and FLO-1 cells were injected subcutaneously into the left and right flanks, respectively, of n = 15 NOD/SCIDγ mice and allowed to implant for 5 days before the start of daily intraperitoneal treatment with fostamatinib R788. Cages of n = 5 animals were divided into 40 mg/kg R788, 80 mg/kg R788, or vehicle (carboxymethylcellulose [CMC])-only treatment groups, as previously reported by Suljagic et al,[33] and tumors were measured by calipers every 3 days until maximal humane end points were reached, in this case when tumors reached 1500 mm^3 in any direction, which occurred by 33 days. All authors had access to the study data and reviewed and approved the final manuscript

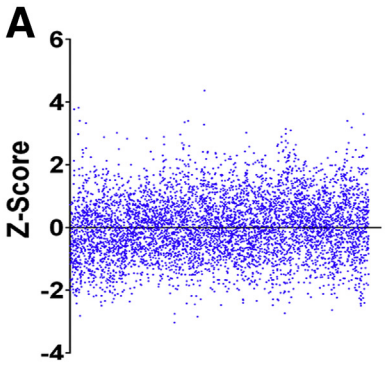

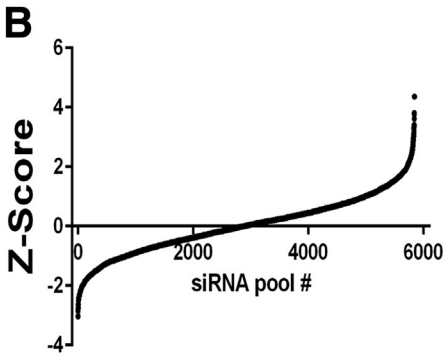

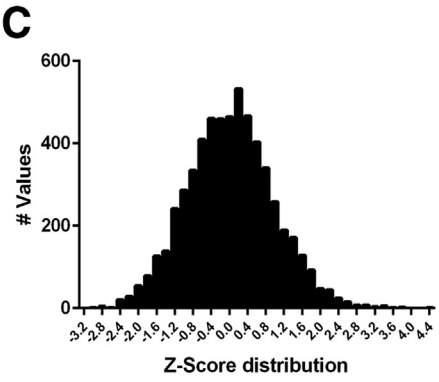

D

Gene	Robust Z Score	Gene	Robust Z Score	Gene	Robust Z Score	Gene	Robust Z Score	Gene	Robust Z Score	Gene	Robust Z Score	Gene	Robust Z Score
UBB	-3.03	RPS29	-2.32	DNAJA2	-2.12	CORO2A	-2.01	C8A	-1.92	NRCAM	-1.83	GDF2	-1.78
RAN	-2.84	RPL37A	-2.29	TADA3L	-2.11	MMAB	-2.01	HIRIP3	-1.92	KRTHB1	-1.83	SPAG1	-1.78
F8	-2.82	TREM2	-2.29	BCL9	-2.11	MYBL2	-2.00	SIGLEC11	-1.92	HSFY2	-1.83	NFKBIL2	-1.78
UBC	-2.75	CCDC6	-2.29	SAMSN1	-2.11	PSMD7	-1.99	PRKAB1	-1.92	WFS1	-1.83	ETF1	-1.77
TPM1	-2.73	TGFB1	-2.29	FOXG1C	-2.10	NPTXR	-1.99	TFAP2C	-1.91	POLH	-1.83	CLCA2	-1.77
GTF2H4	-2.63	TP53	-2.28	TBL1X	-2.10	CDY1	-1.99	GUCA1B	-1.91	PSMA2	-1.83	C1QA	-1.77
RPL5	-2.49	EHF	-2.27	PKP1	-2.09	ABCC10	-1.99	PHC1	-1.91	RAI1	-1.83	RAPGEF6	-1.77
SYMPK	-2.49	PTMA	-2.26	CSEN	-2.09	GPC3	-1.98	SCYE1	-1.91	KNTC2	-1.83	SSR4	-1.76
SRPR	-2.48	SDHD	-2.25	NR1H2	-2.09	HNRPUL1	-1.98	NDP52	-1.89	CLPP	-1.82	ANXA9	-1.76
RAD51	-2.47	KCNAB1	-2.23	UBA52	-2.08	TF	-1.98	GLIS2	-1.89	FRS3	-1.82	JJAZ1	-1.75
AOX1	-2.44	SLC14A1	-2.22	CARD12	-2.08	ETV7	-1.98	PNMT	-1.89	K-ALPHA-1	-1.82	PEX13	-1.75
RPL10	-2.43	CD2BP2	-2.22	DSG3	-2.07	CETN3	-1.98	KIF2C	-1.88	ITGB3	-1.81	RDX	-1.75
CLASP1	-2.42	PDCD2	-2.20	ATF6	-2.06	CANX	-1.97	APBB3	-1.88	TG	-1.81	SEC14L3	-1.75
CORO1C	-2.42	LPL	-2.19	RPL11	-2.06	CYP2D6	-1.97	BAIAP3	-1.88	SGCA	-1.81	PPM1E	-1.75
POLR2A	-2.42	CIRBP	-2.19	TUBGCP3	-2.05	GABRB2	-1.96	DUX1	-1.88	PON3	-1.81	DLX3	-1.75
SH3KBP1	-2.40	SYNJ1	-2.19	RELA	-2.05	TRPM3	-1.96	SERTAD2	-1.87	COL10A1	-1.81	CIZ1	-1.74
TRPC7	-2.40	ISGF3G	-2.18	MAFK	-2.05	SH2D3A	-1.96	ATF5	-1.86	GFRA4	-1.81	TRIP3	-1.74
KCNQ2	-2.39	RPL13A	-2.18	ZNF278	-2.05	VPS52	-1.95	DSPP	-1.86	BIRC7	-1.80	USP18	-1.74
CTCF	-2.39	SVIL	-2.18	KCND3	-2.05	NYX	-1.95	DNTT	-1.86	RLN2	-1.80	PCDHA13	-1.74
SON	-2.38	RABGEF1	-2.17	CDC25C	-2.04	DUSP9	-1.95	HIP2	-1.85	TRAF2	-1.79	GATA1	-1.74
RUNX2	-2.37	FOSL1	-2.15	USP30	-2.04	LIF	-1.95	RABL2B	-1.85	HERC5	-1.79	MAD	-1.73
ITGB6	-2.34	CDH16	-2.15	CFL1	-2.04	IL22	-1.95	LGALS3BP	-1.84	FOSB	-1.79	IL2RA	-1.73
ZNF325	-2.34	GPAA1	-2.13	MLLT6	-2.03	SIX6	-1.95	CPT2	-1.84	NDE1	-1.79	EGR1	-1.73
TRPV2	-2.33	MSH6	-2.13	THBS2	-2.03	CYBA	-1.95	MAPT	-1.84	MEP1B	-1.78	IFNW1	-1.73
KRT10	-2.32	HEY1	-2.12	ALX4	-2.02	MYL7	-1.93	CASP10	-1.83	PROS1	-1.78	FUSIP1	-1.73

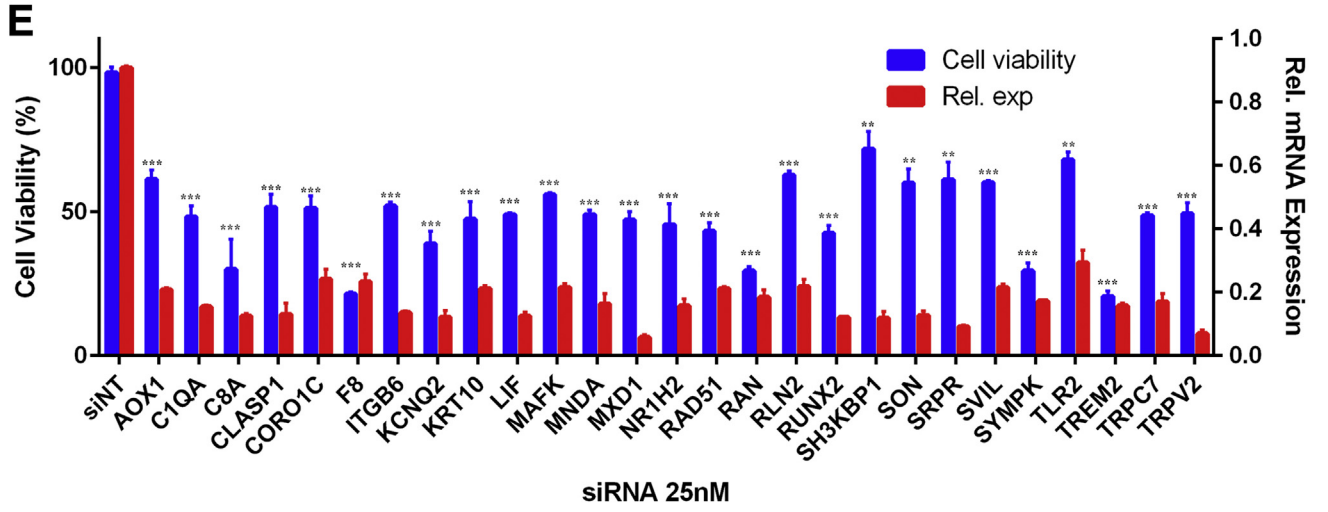

Statistical Analysis

The Student *t* test was used for statistical analysis of biologically replicated (N = 3) functional experiments. Nonparametric Mann–Whitney testing was used for analysis of significance in real-time gene expression experiments performed with both biological (N = 3–23) and technical replicates (N = 3).[18,19,25] The performance of high-throughput screening was determined through the use of a Z-factor quality metric.[34] Statistical interpretation of siRNA screening results was achieved through Z score ranking of normalized median values. One-way analysis of variance and linear regression was used in significance testing of murine xenograft studies performed with GraphPad Prism software (La Jolla, CA).

Results

Druggable Genome Screening of EAC Cell Growth After siRNA-Mediated Silencing

Previous publications from our laboratory showed that silencing of the GATA6 transcription factor resulted in significant EAC cell growth arrest and apoptosis.[25] Positive and negative controls were tested for reproducibility in mock screening protocols. siRNA pools targeting GATA6 were used as a positive control in siRNA library screening of cell viability using the high-grade dysplastic (HGD) cell line CP-D, which reflects many of the pathways of activation in the majority of EAC cell lines. A full-scale, high-throughput siRNA library screen of CP-D cell line viability was implemented using a druggable genome siRNA library consisting of 6022 individual gene-targeting siRNA pools after optimization of screening platform and controls. The performance of this screen was assessed through analysis of the reproducibility between positive (siGATA6; n = 3 technical and n = 3 biological per genome library plate [n = 76]) and negative controls (nontargeting siRNA pools), both in the same siGenome sequence format as the druggable genome library. A clear separation of positive and negative controls was achieved resulting in a screening metric Z-factor of 0.67, indicative of high-quality screening performance. The observed viability data derived from the siRNA screen was distributed normally, permitting the use of standard Z score and robust Z score cut-off values of Z < -1.645, resulting in 299 and 252 gene transcript–targeting siRNA pools, respectively, that significantly affected EAC cell viability (Figure 1*A*–*D*). The mRNA transcripts targeted by these siRNAs included nucleic acid binding proteins, signaling molecules, hydrolases, receptors, and cytoskeletal proteins (Figure 1*D*). As might be expected, key nuclear and nucleic acid binding proteins such as RAD51, SYMPK, and RAN, with obvious oncogenic roles, achieved high Z score rankings (Figure 1*D*) supportive of the approach and the quality of the siRNA screen performed. Gene transcripts (n = 30) were selected from within this list at different levels of significance (top, mid, bottom third) for verification of expression (mRNA) in EAC cells and validation of the effects of their silencing in EAC cells using alternate siRNA formats (siON-target-plus) than used in the original siRNA library screen (siGenome) (Figure 1*E*). Good concordance with the original screening data was achieved while using this alternative siRNA format (Figure 1*E*).

Somatic Gene Amplifications Associate With Druggable Genome siRNA-Targeted Genes

The relationship between regulators of EAC cell growth as defined in siRNA screening data and somatic variation observed in EAC and esophageal squamous cell carcinomas (ESCCs), as recently defined by The Cancer Genome Atlas (TCGA) Research Network, was next examined.[10] Somatic variation (SV) at a frequency above 5% in all esophageal cancers was noted in 49 siRNA target genes from the druggable genome screen, at a cut-off value of Z < -1.645 in 2 independent clinical cohorts of esophageal cancers (EAC and ESCC) and gastric carcinomas (gastroesophageal junction and gastric carcinomas), respectively. Distinct clustering of gene-associated amplifications within specific patient samples could be defined through the oncoprint of both sequencing studies that, when curated, resulted in both cancer tissue- and patient-specific SV patterns (Figure 2). Amplifications associated with GTF2H4, GUCA1B, ABCC10, RUNX2, TREM2, POLH, and FRS3, whose silencing reduced the viability of EAC cells in screening data, were specific to EAC rather than ESCC (Figure 2*A*), significantly higher in gastroesophageal junctions than gastric carcinomas (Figure 2*B*), and were all co-encoded at chromosome 6p21.1. The remaining amplifications separated into 2 further clusters (TONSL, GPAA1, and TG; and KCNQ2, BIRC7, and TFAP2C) that were co-located at chromosome 8q24.3 and 20q13.33, respectively, but did not distinguish between

Figure 1. (***See previous page***). **Regulators of cell proliferation and survival in EAC cells as defined by siRNA druggable genome library screening.** The druggable genome siRNA library (siGenome build) was used in conjunction with a high-throughput end point MTT viability assay of using the CP-D cell line as per the Materials and Methods section. The most significant siRNAs/genes/wells resulting in alterations to EAC cell viability were defined through robust Z score ranking (Z < -1.645) which was normally distributed. (*A*) Nonranked Z scores of siRNA pools from siRNA screening ordered according to plate number. (*B*) Z score ranked individual siRNA pools after normalization and removal of substandard wells. (*C*) Normal distribution of Z sore rankings. (*D*) The Z score ranked list of siRNA targeted genes (Z < -1.645) with the strength of the heatmap color corresponding to level of statistical significance. (*E*) A selection of gene targeting siRNAs were validated (N = 3 biological replicates) in CP-D cells in separate independent experiments using an alternate siRNA format (siOn-target plus build), showing good concordance with the original screening data and a significant decrease in the expression of the associated genes (Mann–Whitney $P < .0001$ for all genes tested) by comparison with nontargeting controls (nontargeting siRNA pool [siNT]). Pos ctrl, siRNA targeting GATA6; Neg ctrl, nontargeting siRNA; Rel. exp., relative expression of associated mRNA by real-time reverse-transcription polymerase chain reaction. $^{**}P < .01$, $^{***}P < .001$, in Student's *t* test.

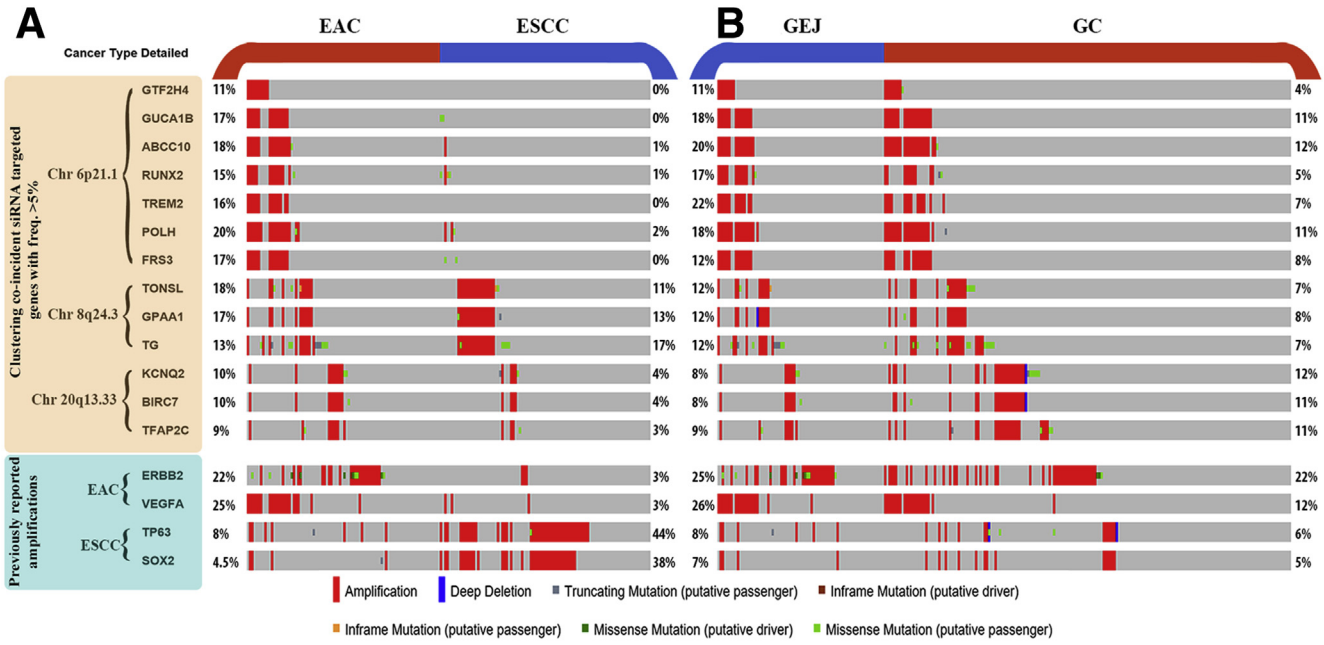
A
B
EAC
ESCC
GEJ
GC
Cancer Type Detailed
Clustering co-incident siRNA targeted genes with freq. >5%
Chr 6p21.1
Chr 8q24.3
Chr 20q13.33
GTF2H4
GUCA1B
ABCC10
RUNX2
TREM2
POLH
FRS3
TONSL
GPAA1
TG
KCNQ2
BIRC7
TFAP2C
Previously reported amplifications
ERBB2
VEGFA
TP63
SOX2
Amplification
Deep Deletion
Truncating Mutation (putative passenger)
Inframe Mutation (putative driver)
Inframe Mutation (putative passenger)
Missense Mutation (putative driver)
Missense Mutation (putative passenger)

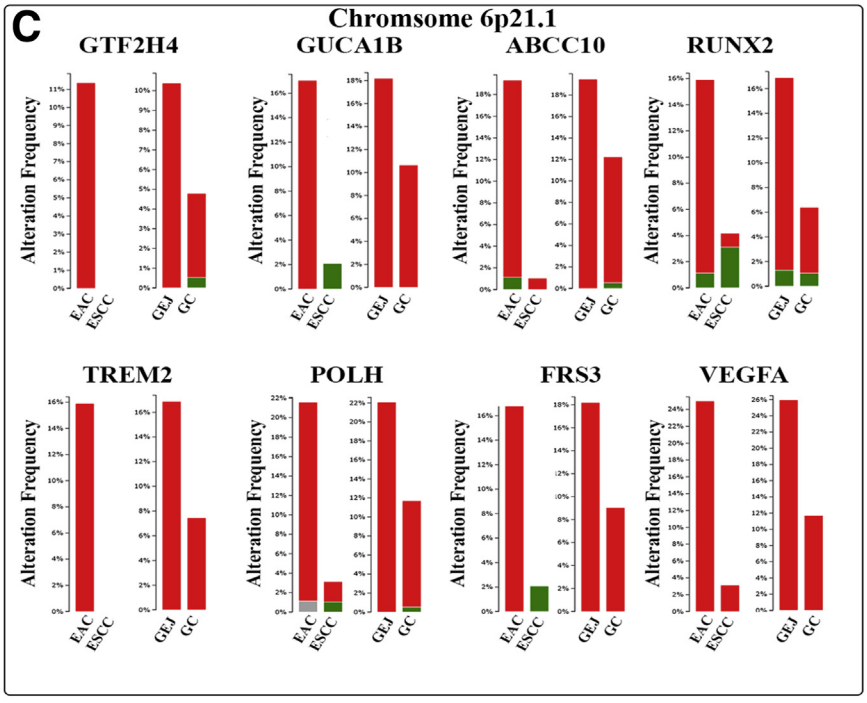
C
Chromsome 6p21.1
GTF2H4
GUCA1B
ABCC10
RUNX2
TREM2
POLH
FRS3
VEGFA
Alteration Frequency
EAC
ESCC
GEJ
GC

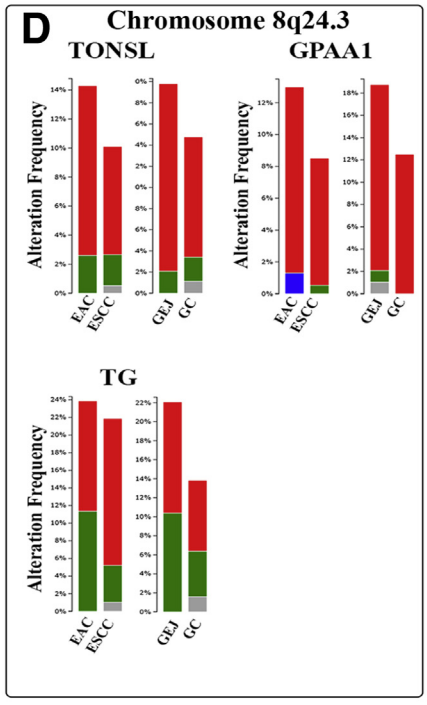
D
Chromosome 8q24.3
TONSL
GPAA1
TG
Alteration Frequency
EAC
ESCC
GEJ
GC

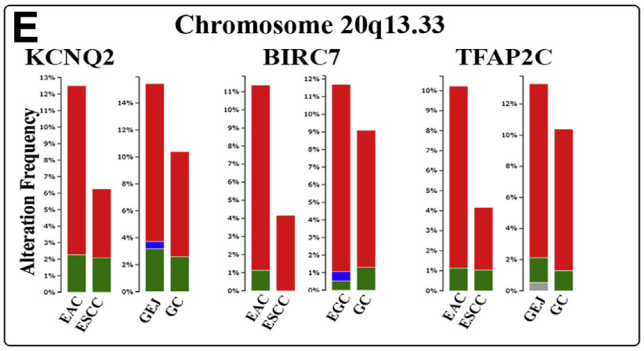
E
Chromosome 20q13.33
KCNQ2
BIRC7
TFAP2C
Alteration Frequency
EAC
ESCC
GEJ
GC


Amplification
Mutation
Deletion
Other

EAC and ESCC cancer types (Figure 2). In total, 12 of 49 somatic events identified clustered at these 3 chromosomal locations. The chromosome location 6p21 is noted for the presence of the immune major histocompatibility complex locus recently associated with the development of BE,[35,36] a precursor to EAC, in genome-wide association studies. Both 8q24.3 and 20q13.33 loci have not traditionally been associated with BE. Comparatively, SV in squamous lineage epithelial cell–associated transcription factors TP63/SOX2, which do not sustain cell growth according to screening data, was associated predominantly with ESCC, as previously described. Conversely, SV in ERBB2 and vascular endothelial growth factor A (VEGFA) was EAC-specific. Thus, results garnered directly from siRNA druggable genome library screening of HGD CP-D cells aligns with the genomic fingerprint observed in genomic studies of EAC and further supports the argument that these events may occur early in the EAC cancer sequence and are specific to EAC over ESCC. It further highlighted chromosomal changes occurring at noted immune-associated loci in a significant number of patients.

Innate-Immune Lymphoid Factors Are Enriched Gene Ontologies Supporting EAC Cell Growth

We subsequently used gene ontologies to identify the gene/protein/pathways predominantly enriched, as regulators of EAC cell growth, within the siRNA library screening data. Cytoscape and the associated plug-in ClueGO[37] were next used to explore gene ontology (GO) enrichments and biological networks within siRNA screening data with a robust Z score cut-off value of $Z<-1.645$ (Figure 1). This resulted in 202 GO terms defining the linked biological processes associated with these genes and accordingly were used further to derive the top-level relationships between the GOs based on the similarity of their associated genes. This process showed the significant presence of 6 immune-related GO clusters from a total of 10 network nodes (Figure 3). The most significant biological processes were those related to cytokine-mediated signaling pathways and cellular responses to molecules of bacterial origin, which together represented 52% of all total relationships (Figure 3). Further validation of these findings was achieved through similar analyses using the FatiGO module of the Babelomics 5.0 platform for functional interpretation of genomics, resulting in broadly similar immune associations (data not shown). These approaches commonly emphasized a distinct and significant over-representation of immune system processes within the genes positive for regulation of CP-D cell growth. Secreted immune factors included C1QA, LIF, IL22, TGFB1, TGFB2, PROK1, THSB2, and CSF3. Membrane-bound immune factors included TREM2, TLR2, IL9R, ITGB3, ICAM1, and TNFRSF8. Cytoplasmic factors with immune relationships included NLRC4, TRAF2, and GAB2. Nuclear immune-related proteins included RELA, RUNX2, NR1H3, EGR1, CTCF, FOSL1, GATA1, MNDA, and BCL6. GERD-induced inflammation has long been associated with the development of esophageal metaplasia and EAC-associated factors.[38] Furthermore, recent evidence has proposed that low-grade epithelial inflammatory responses without inflammatory cell infiltrates, para-inflammation, may be induced by persistent tissue stress and contribute to cancer promotion in murine models.[39,40] Thus, the observed immune-pathway associations observed in CP-D cells may reflect the inflammatory origins of this disease.

Overexpression of LIF, C1QA, and TREM2 in the BE-Associated Cancer Sequence

To examine the expression levels and thus targetability of the genes defined from siRNA library screening, we performed an integrative re-analysis of EAC gene expression microarray (GEM) studies, using methods previously described[25] (Figure 4*A*). This approach highlighted 62 siRNA-targeted genes that are putatively overexpressed in EAC tissues including immune-associated genes C1QA, TREM2, LIF, TGFB1, THBS2, HLA-G, HLA-DQB1, GDF15, IL32, IL15RA, C1S, ICAM1, and TRAF4. When this list is ranked by the strength of effects on EAC cell viability in siRNA screening data, 3 secreted factors were prominent within this list: LIF, C1QA, and triggering receptor expressed on myeloid cells (TREM2) (Figure 4*B*). Secreted factors may have future theranostic potential and thus were an important focus of this study. JAK-STAT signaling pathways, which are activated by IL6 and its family member LIF, have been shown to regulate C1q production in macrophages.[41–43] Both C1Q and TREM2 mediate signaling events through TYROBP(DAP12)-SYK pathways and are associated commonly with innate and chronic inflammatory conditions.[44–46] Higher levels of LIF, C1QA, and TREM2 mRNA were observed in BE and EAC biopsy specimens when compared with squamous control tissues using an independent clinical cohort ($P < .0001$, Mann–Whitney) (Figure 4*C–E*). There are currently no sufficiently accessible databases of EAC patient GEM data with associated survival outcomes. However, a significant association between LIF ($P = 5.4E^{-4}$), C1QA ($P = 3.7E^{-7}$), and TREM2

Figure 2. (*See previous page*). Overlap between EAC-associated somatic variation and siRNA-targeted genes defined by druggable genome siRNA library screening of EAC cells. (*A*) TCGA data charting SV in EAC and ESCC viewed through a curated oncoprint of 13 siRNA-targeted genes with a Z score < -1.645 in screening data and a frequency of SV > 5%, selected for co-enrichment and clustering of the gene amplification events as determined by GISTIC through cBioportal (http://www.cbioportal.org/index.do). (*B*) Parallel analysis of TCGA data containing gastroesophageal junctional (GEJ) and GCs results in similar clustering of gene amplifications events in subsets of both of these tumors types. Amplification events of siRNA-targeted genes that altered EAC cell growth as per druggable genome screening data encoded at chromosome (*C*) 6p21.1, (*D*) 8q24.3, and (*E*) 20q13.33.

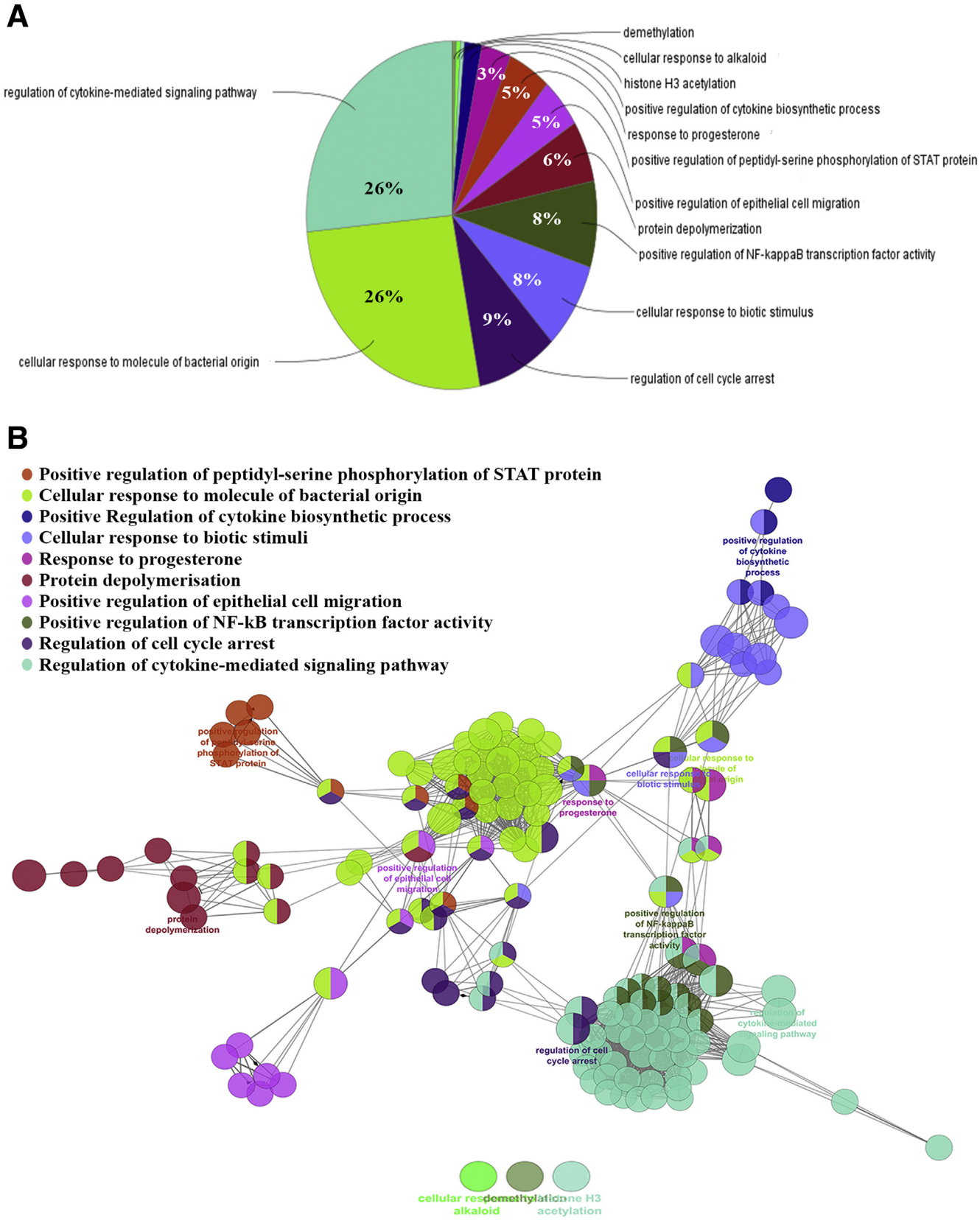

Figure 3. Gene ontology analysis of siRNA screening data. (*A*) ClueGO gene function clustering of gene ontologies, associated with siRNA gene targets, defines significant linkage to cytokine-mediated signaling pathway and cellular response to molecule of bacterial origin from the list of gene-targeting siRNAs defined in Figure 1. (*B*) GO networking of ClueGO results details the overlaps and interactions between the functional groupings. NF-κB, nuclear factor κB.

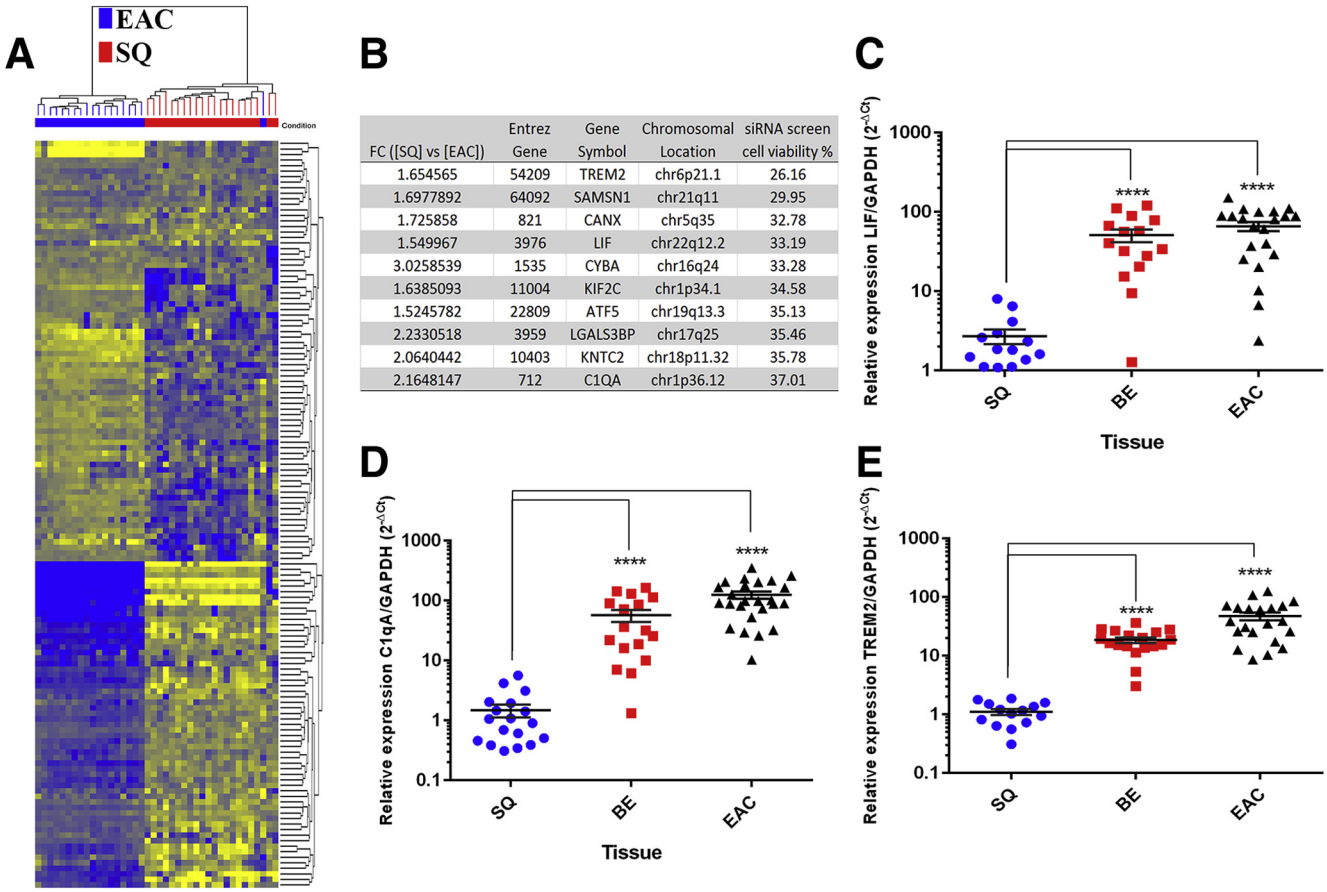

FC ([SQ] vs [EAC])	Entrez Gene	Gene Symbol	Chromosomal Location	siRNA screen cell viability %
1.654565	54209	TREM2	chr6p21.1	26.16
1.6977892	64092	SAMSN1	chr21q11	29.95
1.725858	821	CANX	chr5q35	32.78
1.549967	3976	LIF	chr22q12.2	33.19
3.0258539	1535	CYBA	chr16q24	33.28
1.6385093	11004	KIF2C	chr1p34.1	34.58
1.5245782	22809	ATF5	chr19q13.3	35.13
2.2330518	3959	LGALS3BP	chr17q25	35.46
2.0640442	10403	KNTC2	chr18p11.32	35.78
2.1648147	712	C1QA	chr1p36.12	37.01

Figure 4. LIF, C1QA, and TREM2 mRNA expression in the EAC cancer sequence. (*A*) Hierarchical gene and condition clustering of siRNA gene targets (Z-score < –1.645 in siRNA library screening data) and tissues (EAC and squamous control tissues [SQ]) respectively, in gene expression microarray data ($P < .001$ in moderated *t* test and FC > 1.5) as previously reported.[25] *Blue* and *red* dendrites of conditional clustering signify EAC and SQ tissues respectively. Heat map *yellow* and *blue* coloring denote low and high expression levels respectively. In hierarchical clustering GEM data yellow and blue coloring reflects low and high expression respectively. (*B*) Top 10 genes overexpressed in EAC tissues ranked by the strength of effect achieved in siRNA screening data (robust Z score). Real-time reverse-transcription polymerase chain reaction analysis of (*C*) LIF, (*D*) C1QA, and (*E*) TREM2 mRNA expression in normal esophageal (SQ), BE, and EAC tissues. ****$P < .0001$ in Mann–Whitney testing for differences in mRNA tissue expression. GAPDH, glyceraldehyde-3-phosphate dehydrogenase.

($P = 5.5E^{-6}$) GEM expression pattern and patient survival could be observed in lung adenocarcinoma ($P = 6E^{4}$; $P = .05$), with no associations in squamous lung, ovarian, or breast carcinomas as viewed through the kmplot database. Similarly LIF and C1QA, but not TREM2, expression was associated with poor outcome in gastric adenocarcinoma (www.kmplot.com).[47] The expression of LIF, C1QA, and TREM2 as novel esophageal associations was next localized by immunohistochemistry in BE and EAC tissues (Figure 5). Normal squamous esophageal tissue showed negligible expression of LIF, C1QA, and TREM2, with some expression in the underlying lamina propria and local immune cells (Figure 5). By comparison, consistent and strong staining of LIF, C1QA, and TREM2 was observed in the glandular epithelial cells and surfaces of BE in addition to isolated lymphoid cells within the interstitial spaces (Figure 5). Similarly, strong staining of LIF, C1QA, and TREM2 was observed in EAC tissues (Figure 5), further validating the preceding findings at the mRNA level.

LIF Maintains EAC Cell Survival, Constitutive Levels of phospho-STAT3, IL6, and C1QA

Previous work from our laboratory has shown that LIF was specifically produced by EAC cells in response to bile acid exposure with no such induction observed in squamous cell lines.[18] In more recent murine models of esophageal dysplasia, reduced levels of dysplastic lesions have been observed in *Il-6* and *Il-1b* double-knockout mice, implicating the IL6-STAT3 pathway in supporting EAC development.[48] The involvement of LIF, an IL6 family member, in EAC oncogenesis has not been explored. Thus, we next studied the role of LIF signaling in EAC cell lines. Silencing of LIF in multiple EAC cell lines resulted in significantly reduced levels of target mRNA (Figure 6*A*),

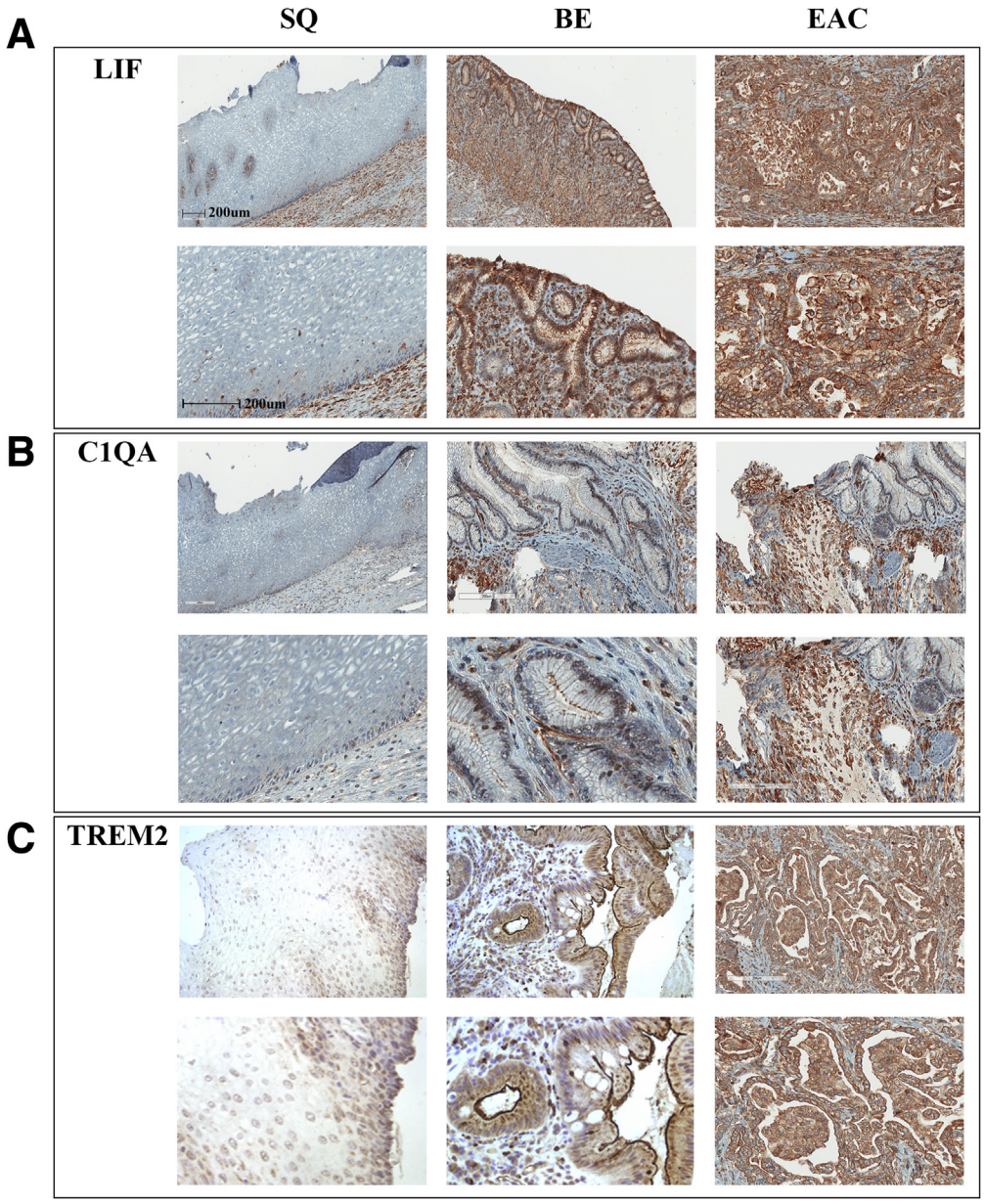

Figure 5. Immunohistochemistry confirms expression of LIF, C1QA, and TREM2 in BE and EAC tissues. Immunohistochemical staining pattern of (*A*) LIF, (*B*) C1QA, and (*C*) TREM2 in normal squamous (SQ), BE, and EAC tissues showing glandular membranous and perinuclear expression in epithelial cells in addition to expression by infiltrating or resident immune cell types. Images are from digitally zoomed fields of view from scanned slides using ImageScope (Leica). *Original magnification*: top, 10×; bottom, 20×.

secreted LIF protein (Figure 6*B*), and reduced cell viability in multiple EAC cell lines (Figure 6*C*), as suggested from siRNA screening data. The lower proliferative rate of LIF-silenced EAC cells could be returned to normal levels by treatment with recombinant LIF protein (Figure 6*C*), which was associated with re-expression of LIF mRNA (Figure 6*D*), LIF protein (Figure 6*E*), and a consequent return of constitutive phospho-STAT3-Y705 levels in EAC cells (Figure 6*F*). Treatment of resting EAC cells with exogenous LIF marginally induced IL6 mRNA levels, with no alterations under treatment with recombinant IL6 protein (Figure 6*G*). Importantly, substantially reduced levels of IL6 mRNA (80%, *t* test $P < .001$) were observed in LIF-silenced EAC cells, which could be returned to basal levels when treated with either exogenous recombinant LIF or recombinant IL6 protein (Figure 6*G*). Thus, silencing LIF overproduction by EAC cells allows the STAT3 pathway to once again become responsive to exogenous IL6 or LIF. This renewed responsiveness to exogenous IL6 could be blocked through the use of an IL6-blocking antibody, resulting in lower levels of target IL6 mRNA transcript (Figure 6*G*). However, siRNA- and blocking antibody–mediated inhibition of IL6 action in LIF-silenced cells did not result in any significant effects on EAC cell growth or LIF levels (Figure 6*H*), placing LIF hierarchically above IL6 expression and STAT3 activation in EAC cell lines. Because LIF, C1q, and TREM2[49] are all secreted factors it is likely that their pathways may converge in the maintenance of continued EAC cell growth. During validation of LIF silencing, reduced levels of C1QA mRNA were observed in LIF-silenced EAC

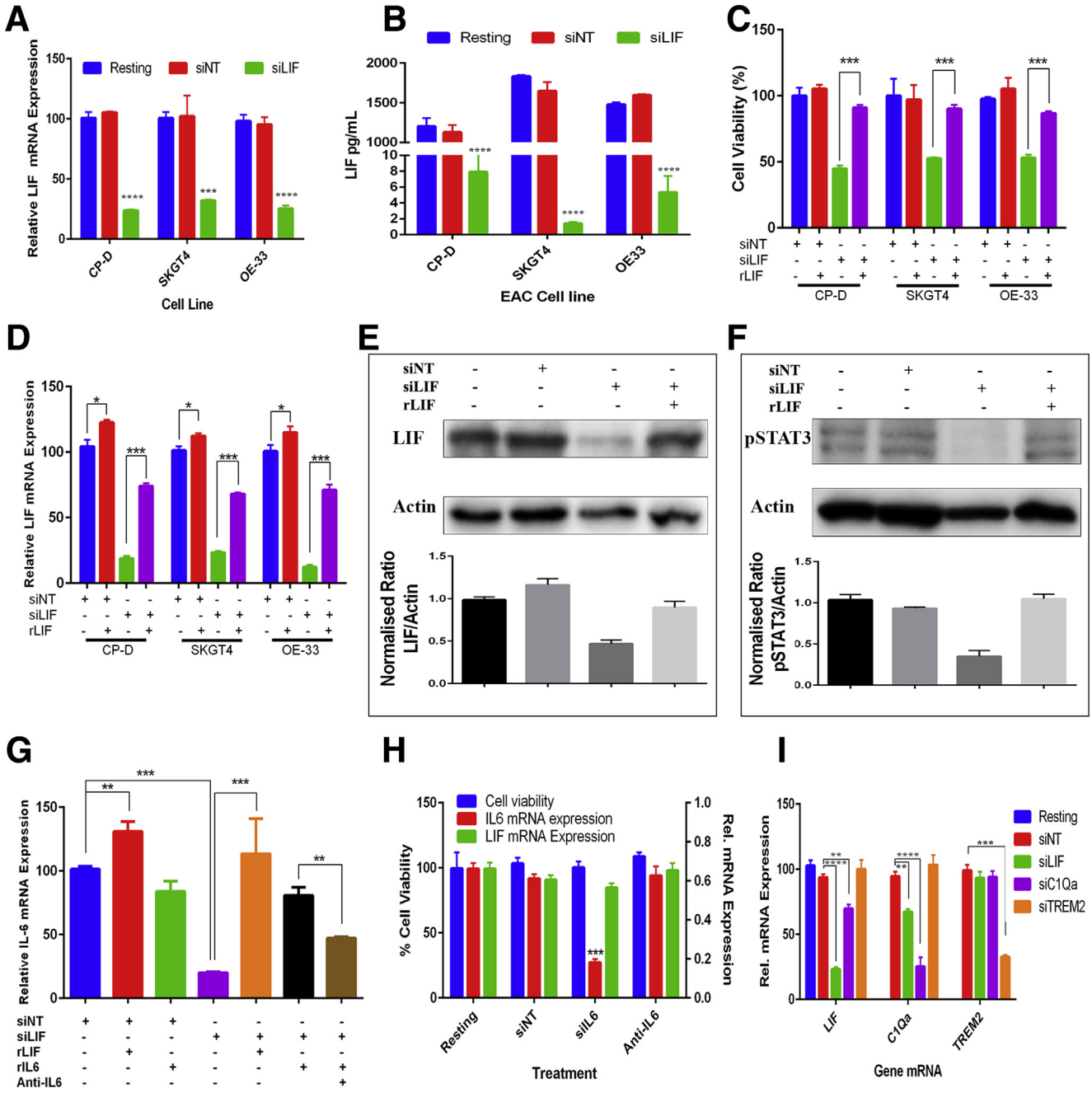

Figure 6. LIF hierarchically regulates STAT3 phosphorylation, IL6 expression, and cell proliferation in EAC cells. SiRNA-mediated silencing of LIF expression results in reduced LIF mRNA (*A*) expression, (*B*) secretion, and (*C*) a recombinant-recoverable reduction in cell proliferation in CP-D, SKGT4, and OE-33 EAC cell lines. Treatment of LIF silenced cells with recombinant LIF protein (rLIF) results in (*D*) recovery of LIF mRNA in CP-D, SKGT4, and OE33 EAC cells and (*E*) protein expression levels in SKGT4 EAC cells. (*F*) STAT3-Y705 phosphorylation levels in LIF-silenced SKGT4 EAC cells are rescued by treatment with recombinant LIF protein as determined by Western blot. (*G*) Silencing LIF expression in SKGT4 EAC cells results in decreased IL6 mRNA expression that is recovered upon exposure to rLIF protein. (*H*) Neither silencing IL6 expression by siRNA-mediated silencing nor treatment with anti-IL6 antibody affects LIF mRNA levels or SKGT4 EAC cell growth. (*I*) Silencing LIF expression results in decreased expression of C1QA mRNA but not TREM2 in SKGT4 EAC cells. $^{*}P < .05$, $^{**}P < .01$, $^{***}P < .001$, and $^{****}P < .0001$ in either Student *t* test (proliferation) or Mann–Whitney testing (mRNA expression). siNT, nontargeting siRNA pool; siLIF, LIF-targeted siRNA pool; rLIF, recombinant LIF protein; rIL6, recombinant IL6 protein.

cells (Figure 6*I*), consistent with the reported STAT3 regulation of C1q production in macrophages.[42,43,50] Similarly, reduced levels of LIF mRNA expression were observed in C1QA-silenced EAC cells, with no detectable changes in TREM2 levels under either conditions (Figure 6*I*). Thus, a partial interdependence between LIF and C1QA mRNA levels was uncovered, suggestive of overlap between these pathways.

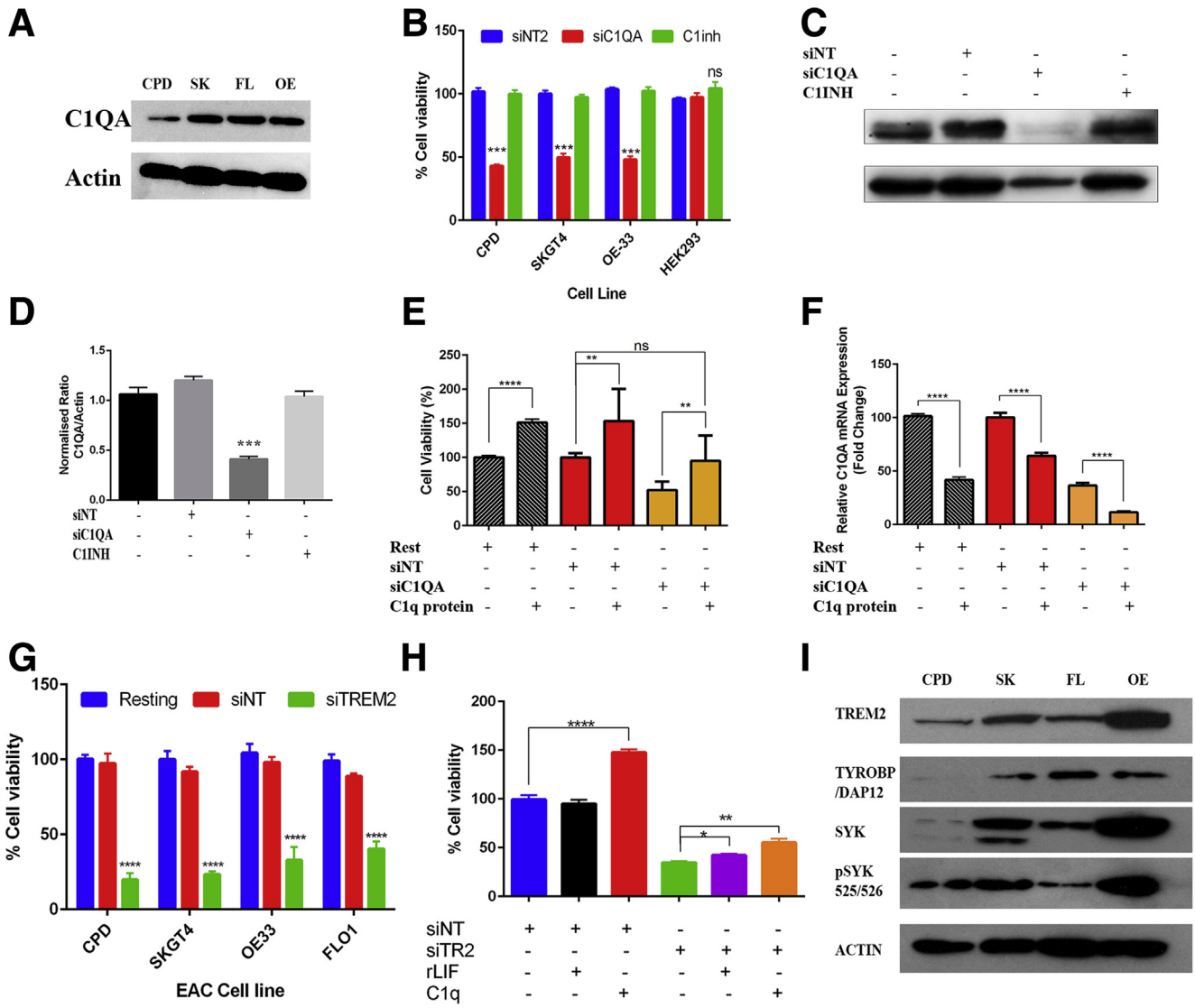

Figure 7. C1q is produced by EAC cells and promotes cell proliferation in an autocrine manner. (*A*) Expression of C1QA protein in EAC cell lines by Western blot. (*B*) Silencing of C1QA results in reduced EAC cell viability with no effects on HEK-293 cells. (*C*) C1QA protein expression by Western blot after siRNA-mediated silencing or treatment with C1 inhibitor protein $C1_{INH}$ in SKGT4 EAC cells. (*D*) Densitometry of panel *C*. (*E*) Cell viability and (*F*) C1QA mRNA levels in SKGT4 EAC cells after either silencing of C1QA or treatment of siC1QA-silenced cells with native C1q to examine recovery of proliferative phenotypes. (*G*) Cell viability of multiple EAC cell lines after siRNA-mediated silencing of TREM2. (*H*) Treatment of TREM2-silenced SKGT4 EAC cells with rLIF or C1q native protein resulted in the rescue of the observed growth arrest. (*I*) Expression of TREM2 and C1q-associated ITAM docking protein TYROBP (DAP12), signaling intermediary SYK and p-SYK in multiple EAC cell lines. $^{**}P < .01$, $^{***}P < .001$, and $^{****}P < .0001$ in either Student *t* test (proliferation) or Mann–Whitney testing (mRNA expression). siC1QA, siRNA pools targeting complement C1q subcomponent subunit A; siNT, nontargeting siRNA pool; siTREM2, siRNA pools targeting triggering receptor expressed on myeloid cells 2.

Autocrine Non–Complement-Mediated Promotion of EAC Cell Growth by C1q

A growing body of evidence suggests nonhumoral immune roles for complement proteins such as C1q-mediated activation of Wnt signaling pathways in epithelial cells.[51–53] The expression of C1QA was next examined in multiple EAC cell lines by Western blot (Figure 7*A*). Post screen verification experiments showed that inhibition of C1QA by siRNA-mediated silencing results in reduced cell growth of the CP-D cell line. This was confirmed further in a wider panel of additional EAC cell lines shown to express C1QA protein, with no effects observed in HEK293 cells that express limited levels of C1q protein (Figure 7*B*). Inhibition of traditional C1q complement function through exposure of EAC cells to $C1_{INH}$ did not result in any observable effect on EAC cell growth (Figure 7*B*) or expression levels (Figure 7*C* and *D*) by comparison with siRNA-mediated silencing of C1QA expression. Critically, the reduced levels of cell growth observed in C1QA-silenced EAC cells (42%; $P < .001$) could be returned to normal levels (98%, $P =$ NS) after treatment

with native C1q protein (Figure 7*E*), indicative of the involvement of a distinct non–complement-mediated signaling mechanism in response to C1q protein. Strikingly, treatment of resting and nontargeting control-transfected EAC cells with native C1q protein resulted in increased EAC cell proliferation (Figure 7*E*). These data are supportive of an autocrine C1q-driven cell survival/growth mechanism in EAC. During validation of C1QA mRNA levels in transfected cells it was also discovered that treatment of resting and C1QA-silenced EAC cells with native C1Q protein results in a feedback-like mechanism, leading to reduced levels of C1QA mRNA transcript (37%, $P < .001$; 11.5%, $P < .001$ resting and siC1QA, respectively) (Figure 7*F*). This further supports the presence C1q-mediated signaling pathways in EAC cells promoting cell growth and control of localized C1q production.

TREM2 and Its Associated Signaling Pathway Regulates EAC Cell Survival

TREM2 is a transmembrane and secreted factor, and similar to C1q, recently has been associated with Alzheimer's disease, innate and humoral immune responses, and triggering constitutive production of cytokines through the TYROBP (DAP12) adaptor protein.[54,55] TREM2 mRNA expression directly correlates with that of C1QA ($r_s = 0.69$), C1QB ($r_s = 0.71$), C1QC ($r_s = 0.72$), and the ITAM adapter protein TYROBP ($r_s = 0.73$) expression in EAC tissues using TCGA data. Validation of TREM2-mediated support of EAC cell growth was next performed in a wider panel of EAC cell lines transfected with TREM-2 targeting siRNAs, confirming similar suppression of cell growth as observed in the original screen and post screen verification (Figure 7*G*). No significant effects on the expression of TREM2 were noted in LIF- or C1QA-silenced cells (Figure 6*I*). However, treatment of TREM2-silenced SKGT4 EAC cells with either recombinant LIF or native C1q proteins resulted in a statistically significant rescue of cell viability (Figure 7*H*). TREM2, in a similar fashion to C1q, may mediate cell signaling through immunoreceptor tyrosine-based motif proteins such as TYROBP, leading to downstream SYK pathway activation in a variety of cell types.[44,45,56] In Western blot experiments, TREM2, TYROBP (DAP12), SYK, and phospho-SYK expression was validated in a panel of EAC cell lines showing the presence of the associated signaling pathway in esophageal cell lines (Figure 7*I*).

Targeting the Immune Signature of EAC Cells With Fostamatinib

SYK inhibitors such as fostamatinib (R788 prodrug; R406 active format) have shown promise in treating allergic and autoimmune conditions, such as rheumatoid arthritis (RA), in addition to B-cell lineage malignancies.[57–60] However, numerous SYK inhibitors display incomplete specificity for SYK, as is the case for most adenosine triphosphate–competitive kinase inhibitors.[61] The SYK inhibitor fostamatinib has been shown to additionally inhibit kinases such as JAK2 and JAK3,[61] both of which communicate signaling from LIF and IL6 through the STAT3 transcription factor. Because LIF, C1q, and TREM2 signaling were prominent in the regulation of EAC cell survival/growth, we examined the ability of fostamatanib R406 to target the JAK/STAT and SYK/AKT pathways and induce growth arrest or apoptosis in EAC cells. Under increasing doses of R406 a significant decrease in both STAT3 and AKT phosphorylation was observed in SKGT4 EAC cells as determined by the phospho/total protein ratio in enzyme-linked immunosorbent assays (Figure 8*A*) and via Western blot of phospho-STAT3 and phospho-AKT (Figure 8*B*). Furthermore, significant levels of apoptosis (18.7% ± 1.7 sub-G0/G1 or R6; $P < .001$), as defined by 7-AAD/bromodeoxyuridine staining, were observed in SKGT4 cells treated with 12.5 μmol/L R406 by comparison with vehicle control (3.8% ± 0.87 sub-G0/G1 or R6) in addition to increased growth arrest (31.5% ± 2.3 G0/G1; $P < .001$) at 24 hours (Figure 8*C* and *D*). These findings were replicated in EAC cell lines known to form robust tumors in nude mice, OE33 cells, and FLO-1 cells over a range of R406 concentrations and measuring cell proliferation and apoptosis at 24 hours (Figure 8*E*). To further show the efficacy of fostamatinib for therapeutic use, OE33 (left flank) and FLO1 (right flank) cells were allowed to engraft in NOD/SCIDγ mice for 5 days before segregation into treatment groups (n = 5) for daily injection of vehicle or fostamatinib R788 prodrug at 40-mg/kg and 80-mg/kg treatment. Significantly reduced tumor volumes were achieved for both cell lines (linear regression $P < .0001$) in both treatment groups, with no significant difference between 40-mg/kg and 80-mg/kg doses. Over the first 30 days after engraftment, treatment with 80 mg/kg R788 significantly suppressed tumor growth, however, some evidence of refractory growth pattern in response to the fostamatinib R788 inhibitor was observed at day 33 (Figure 8*F*).

Discussion

Herein, we define a cohort of targetable factors whose siRNA-mediated silencing inhibited EAC cell growth. Critically, we also show that somatic variation observed in EAC directly associates with genes sustaining EAC cell growth as defined by siRNA library screening. The screening approach, although only completed in CP-D HGD cells, however, resulted in significant findings that could be verified through pathologic and functional studies using both alternate siRNA formats, recombinant proteins, and rescue experiments supporting the overall immune-signature associations described herein. EAC develops in a background of GERD-induced inflammation and it recently was postulated that inflammatory factors may be directly responsible for the induction of metaplasia development rather than a process of caustic erosion followed by metaplastic replacement.[17] Furthermore, a growing body of evidence has defined the epithelial-autonomous activation of inflammatory responses termed *parainflammation* in mice,[39,40,62] human beings,[39] and numerous carcinoma cell lines.[39] The data suggest that the low-grade epithelial inflammation induced by a stressor in conjunction with

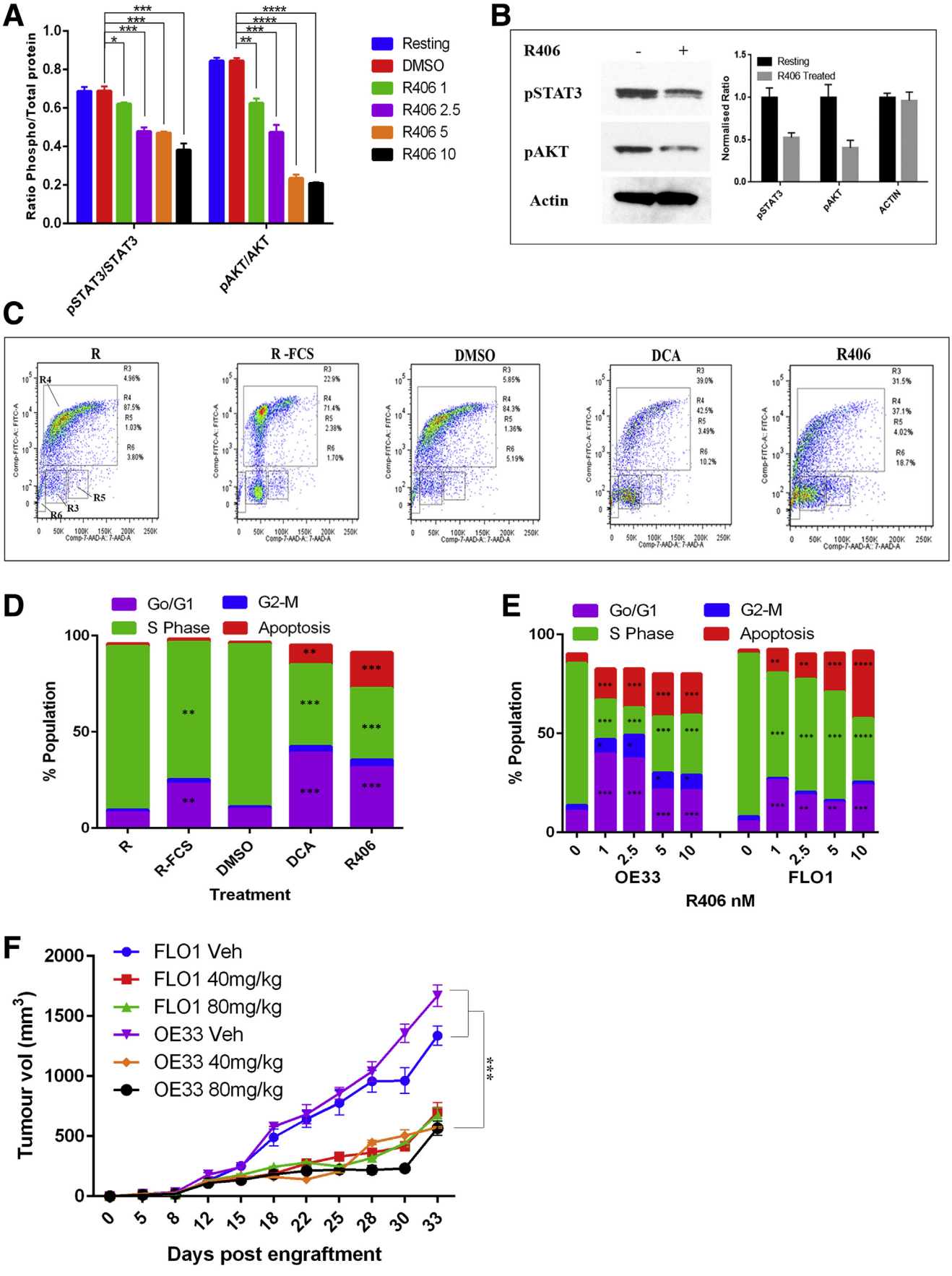
A
Ratio Phospho/Total protein
pSTAT3/STAT3
pAKT/AKT
Resting
DMSO
R406 1
R406 2.5
R406 5
R406 10
B
R406
pSTAT3
pAKT
Actin
Normalised Ratio
Resting
R406 Treated
pSTAT3
pAKT
ACTIN
C
R
R -FCS
DMSO
DCA
R406
D
Go/G1
S Phase
G2-M
Apoptosis
% Population
R
R-FCS
DMSO
DCA
R406
Treatment
E
Go/G1
S Phase
G2-M
Apoptosis
% Population
OE33
FLO1
R406 nM
F
FLO1 Veh
FLO1 40mg/kg
FLO1 80mg/kg
OE33 Veh
OE33 40mg/kg
OE33 80mg/kg
Tumour vol (mm3)
Days post engraftment

tumor-suppressor loss (p53 mutation) results in a macrophage mimicry by tumor cells.[40,62] In addition, recent sequencing studies have defined glioblastoma subsets with distinct complement response signature derived from CD45-depleted tumors.[63] Our detection of an enriched immune signature underlying the promoters of EAC cell viability as determined by siRNA library screening, thus is supported by considerable evidence. Moreover, nuclear proteins guiding genome integrity and mitotic fidelity also were prominent regulators of cancer cell survival, as might be expected, from the siRNA screening data and included SYMPK, RAD51, and RAN, which all were overexpressed in GEM data of EAC. The presence of RAD51 within this list likely reflects the instability associated with the EAC cell genome and previously has been linked with alterations in copy number and heterozygosity in EAC cells.[64–66]

Recent integrative genomic analyses of esophageal and gastric carcinomas, performed as a component of the TCGA project, has characterized the associated somatic and epigenetic alterations to facilitate improved classification and selection of appropriate therapeutic modalities.[10] Carcinoma-specific amplifications defined include ERBB2, VEGFA, and GATA6 in EACs, and TP63, SOX2, and CCND1 in ESCCs. When genes supportive of EAC cell growth as defined through siRNA screening of CP-D cells were examined in TCGA data of esophageal tumors a significant intersection was uncovered composed of 49 genes with somatic frequencies greater than 5%. Intriguingly, 14% (7 of 49) of these genes showing gene amplifications, at similar frequencies to ERBB2 and VEGFA amplifications, were encoded at Chr6p21.1 and specifically associated with EAC rather than ESCC carcinomas. This further supports the hypothesis that the observed somatic variation is occurring in differentiation pathways specific to EAC. Chromosome 6p21 and the major histocompatibility locus in particular has been linked consistently with risk of both BE and EAC in genome-wide association studies and follow-up meta-analyses further supporting the inflammatory links to this cancer type.[35,36,67] As previously reported, VEGFA is similarly encoded at Chr6p.21.1 and initially proposed as a putative target of amplifications at this locus.[10] However, blocking monoclonal antibodies to VEGF such as bevacizumab have been disappointing in clinical trials.[68] Thus, the significant association between genes sustaining EAC growth in siRNA screening data and their expression from Chr6p21.1 supports the hypothesis that alterations at this locus also may contribute to oncogenesis through enhanced proliferative rates in addition to that mediated by alterations to VEGFA levels and angiogenic pathways. Comparatively, no consistent links have been detailed between Chr8q24.3 and Chr20q13.33 and either BE, EAC, or ESCC occurrence genomic studies. No ESCC-specific signature was associated with the 49 gene amplifications highlighted in our study. However, a significant ESCC-specific signature could be defined when squamous markers TP63 and SOX2 were analyzed, although neither SOX2 nor TP63 sustain EAC cell growth according to screening data. Gene amplification events that were defined at Chr8q24.3 and Chr20q13.33 were not cancer-type–specific and occurred at similar frequencies in either EAC or ESCC. Thus, the integration of somatic variation data with druggable genome screening results highlights a significant overlap that supports the validity of the potential targets identified in this study.

Analysis of druggable genome screening results, using multiple GO software platforms,[37,69,70] provided strikingly similar interpretations of the gene-function relationships. These findings indicated the involvement of immune-related pathways in the regulation of EAC cell growth and survival. The development of BE, and by relationship EAC, previously has been associated with GERD-promoted inflammation. Recent reports in murine models have shown that viral-mediated overexpression of *Il1b* in the upper alimentary tract can lead to an *Il6*-dependent Barrett's-like metaplasia, with dysplasia.[48] In our study, neither silencing of IL6 expression nor anti-IL6 blocking affected EAC cell growth or survival in human cell lines. However, silencing of the IL6 family member, LIF, resulted in significantly reduced EAC cell proliferation, pSTAT3 and IL6 levels in SKGT4 EAC cells that could be rescued through treatment with exogenous recombinant LIF. Critically, silencing LIF expression also resulted in reduced C1QA levels, showing an interdependency between these pathways. STAT3 is a known SYK pathway substrate further supporting this finding. Because both C1q and TREM2 similarly use SYK-mediated signaling pathways in immune cell types, these proteins were selected for further analysis.

The C1QA gene encodes a subcomponent of the trimeric C1q complement protein normally associated with the

Figure 8. (***See previous page***). **Targeting SYK and JAK with fostamatinib results in EAC cell growth arrest, apoptosis, and reduced xenografted-tumor burden.** (*A*) Ratio of total STAT or AKT protein to phospho-STAT3 or phosphor-AKT protein after a 90-minute treatment of SKGT4 EAC cells with fostamatinib R406 as measured by enzyme-linked immunosorbent assay. (*B*) Western blot of phospho-STAT3, phospho-AKT after treatment with either dimethyl sulfoxide (DMSO) (-) or R406 10 nmol/L(+). (*C* and *D*) Fluorescence-activated cell sorter analysis of SKGT4 EAC cell-cycle phase after treatment of SKGT4 EAC cells with fostamatinib R406 (active drug), DMSO (vehicle), DCA (positive control), or low FCS media (R-FCS negative control). (*E*) Fluorescence-activated cell sorter analysis of OE33 and FLO1 EAC cell-cycle phase after treatment with a concentration curve of fostamatinib R406. (*F*) Xenografted tumor volume measurements (n = 5) in NOD/SCIDγ mice after engraftment with FLO1 (left flank) and OE33 (right flank) cell lines and daily treatment with either CMC (vehicle) or fostamatinib R788 (prodrug) at 40 or 80 mg/kg. R4, S-phase cell population; R3, G0/G1 phase cell population; R5, G2/M phase cell population; R6, sub-G1 early apoptosis cell population; CMC, carboxymethylcellulose; R, resting; R-FCS, resting cells in culture media without DMSO; R406, active metabolite of SYK inhibitor fostamatinib; R788, fostamatinib, a prodrug of the active metabolite and SYK inhibitor R406. $^{*}P < .05$, $^{**}P < .01$, $^{***}P < .001$, $^{****}P < .0001$ in either Student's *t* test (fluorescence-activated cell sorter and enzyme-linked immunosorbent assay data) or linear regression (R406 xenograft study data in panel *E*). FITC, fluorescein isothiocyanate; Veh, vehicle.

innate surveillance system thought to largely occur from bone marrow–derived cells such as macrophages and dendritic cells.[71] Thus, the expression and production of C1q by EAC epithelial cells, in our study, and its promotion of sustained EAC cell growth through non–complement-pathway–mediated autoregulatory signaling was unexpected. Silencing of the complement C1q binding protein (C1QBP or GC1QR), which normally binds to the globular heads of C1q protein, thus inhibiting C1 activation, has been observed to result in reduced lamellipodia formation and consequently reduced cell migration and invasion of cancer cells in a number of studies.[72,73] However, silencing C1QBP was not observed as a significant regulator of EAC cell growth in our screening data. A clear increase in metaplastic epithelial and luminal cell surface expression of C1QA was observed in tissue sections from BE patients that was mirrored at the mRNA level in both BE and EAC by comparison with squamous control tissues. Similarly, TREM2 immunostaining reflected that observed at the mRNA level. Dense epithelial cytoplasmic and cell surface expression of TREM2 was noted in goblet cell–positive glands of BE and, intriguingly, in putative neuroendocrine cells noted within glandular structures. A number of studies have linked inappropriate activation of both TREM2 and C1Q function independently with the development of Alzheimer's disease through microgliosis and augmented complement-mediated synaptic pruning, respectively, supporting a shared functional relationship between these proteins.[54–56,74–79]

The functions associated with TREM2 have to date remained rooted in immune and neuronal cell types and osteoclasts, with few studies on its role in carcinogenesis. However, recent reports have indicated that silencing TREM2 in glioma cells may result in cell death and thus provide a rational therapeutic target.[80] Unfortunately, no GEM database with associated survival metrics for EAC patients currently exists in a publicly accessible form. However, a significant preferential association between high LIF, C1QA, and TREM2 mRNA expression and poorer survival outcome was defined in such a database of lung and gastric adenocarcinoma patients in our analysis of kmplot data.[81] Treatment of TREM2-silenced EAC cells with exogenous native C1q protein partially rescued EAC cell viability, supportive of a shared signaling pathway. Components of the signaling pathways used by TREM2 and C1q in immune cells, immunoreceptor tyrosine-based activation motif (ITAM) docking protein TYROBP and SYK, were expressed in EAC cell lines. SYK expression also was confirmed in EAC cell lines and was responsive to fostamatinib treatment, resulting in decreased cell cycle S-phase percentages and increased EAC cell death.

The oral SYK inhibitor fostamatinib is currently under clinical and experimental trials for the treatment of a range of conditions such as immune thrombocytopenia, RA,[82] refractory B-cell lymphoma,[59] and glomerulonephritis.[60,83] Limited off-target pharmacologic effects such as increased blood pressure have been noted in early clinical trials.[57,58] Within these pharmacologic studies the specificity for SYK is still quite high but significant effects on kinases such as JAK2 also are observed.[61] The JAK2/STAT3 pathway mediates cytokine induction of receptor activator of nuclear factor kappa-B ligand (RANKL) in synovial fibroblasts in RA and thus combined inhibition of both SYK and JAK by fostamatinib may be beneficial. Importantly, JAK2 is central in mediating responses to IL6 and LIF through IL6R and gp130 cell surface receptors.[84,85] Thus, the use of R788/fostamatinib for the treatment of EAC, as suggested by this report, may mediate therapeutic effects through JAK/STAT and SYK, key pathways in the inflammatory promotion of EAC and the regulation of EAC cell proliferation and survival as defined in this study.

In summation, these findings further show and provide molecular evidence for the involvement of inflammatory factors in the development of EAC. Furthermore, the data provide actionable targets for the development of EAC therapeutics that may support standard chemotherapy-based approaches and provides proof of concept for one such therapeutic target pathway. Although we have focused on the subset of genes associated with the SYK JAK-STAT pathway, further studies will address the additional immunologic pathways uncovered in this study and we anticipate that this approach will uncover further new therapeutic options.

References

1. Thrift AP, Whiteman DC. The incidence of esophageal adenocarcinoma continues to rise: analysis of period and birth cohort effects on recent trends. Ann Oncol 2012; 23:3155–3162.
2. Jemal A, Siegel R, Xu J, Ward E. Cancer statistics, 2010. CA Cancer J Clin 2010;60:277–300.
3. Soontrapornchai P, Elsaleh H, Joseph D, Hamdorf JM, House AK, Iacopetta B. TP53 gene mutation status in pretreatment biopsies of oesophageal adenocarcinoma has no prognostic value. Eur J Cancer 1999;35:1683–1687.
4. Agrawal N, Jiao Y, Bettegowda C, Hutfless SM, Wang Y, David S, Cheng Y, Twaddell WS, Latt NL, Shin EJ, Wang LD, Wang L, Yang W, Velculescu VE, Vogelstein B, Papadopoulos N, Kinzler KW, Meltzer SJ. Comparative genomic analysis of esophageal adenocarcinoma and squamous cell carcinoma. Cancer Discov 2012;2:899–905.
5. Kandioler D, Schoppmann SF, Zwrtek R, Kappel S, Wolf B, Mittlbock M, Kuhrer I, Hejna M, Pluschnig U, Ba-Ssalamah A, Wrba F, Zacherl J. The biomarker TP53 divides patients with neoadjuvantly treated esophageal cancer into 2 subgroups with markedly different outcomes. A p53 Research Group study. J Thorac Cardiovasc Surg 2014;148:2280–2286.
6. Yamamoto Y, Wang X, Bertrand D, Kern F, Zhang T, Duleba M, Srivastava S, Khor CC, Hu Y, Wilson LH, Blaszyk H, Rolshud D, Teh M, Liu J, Howitt BE, Vincent M, Crum CP, Nagarajan N, Ho KY, McKeon F, Xian W. Mutational spectrum of Barrett's stem cells suggests paths to initiation of a precancerous lesion. Nat Commun 2016;7:10380.
7. Chong IY, Cunningham D, Barber LJ, Campbell J, Chen L, Kozarewa I, Fenwick K, Assiotis I, Guettler S, Garcia-Murillas I, Awan S, Lambros M, Starling N, Wotherspoon A, Stamp G, Gonzalez-de-Castro D,

Benson M, Chau I, Hulkki S, Nohadani M, Eltahir Z, Lemnrau A, Orr N, Rao S, Lord CJ, Ashworth A. The genomic landscape of oesophagogastric junctional adenocarcinoma. J Pathol 2013;231:301–310.

8. Dulak AM, Stojanov P, Peng S, Lawrence MS, Fox C, Stewart C, Bandla S, Imamura Y, Schumacher SE, Shefler E, McKenna A, Carter SL, Cibulskis K, Sivachenko A, Saksena G, Voet D, Ramos AH, Auclair D, Thompson K, Sougnez C, Onofrio RC, Guiducci C, Beroukhim R, Zhou Z, Lin L, Lin J, Reddy R, Chang A, Landrenau R, Pennathur A, Ogino S, Luketich JD, Golub TR, Gabriel SB, Lander ES, Beer DG, Godfrey TE, Getz G, Bass AJ. Exome and whole-genome sequencing of esophageal adenocarcinoma identifies recurrent driver events and mutational complexity. Nat Genet 2013; 45:478–486.
9. Streppel MM, Lata S, DelaBastide M, Montgomery EA, Wang JS, Canto MI, Macgregor-Das AM, Pai S, Morsink FH, Offerhaus GJ, Antoniou E, Maitra A, McCombie WR. Next-generation sequencing of endoscopic biopsies identifies ARID1A as a tumor-suppressor gene in Barrett's esophagus. Oncogene 2014; 33:347–357.
10. Cancer Genome Atlas Research Network; Analysis Working Group: Asan University; BC Cancer Agency; Brigham and Women's Hospital; Broad Institute; Brown University; Case Western Reserve University; Dana-Farber Cancer Institute; Duke University; Greater Poland Cancer Centre; Harvard Medical School; Institute for Systems Biology; KU Leuven; Mayo Clinic; Memorial Sloan Kettering Cancer Center; National Cancer Institute; Nationwide Children's Hospital; Stanford University; University of Alabama; University of Michigan; University of North Carolina; University of Pittsburgh; University of Rochester; University of Southern California; University of Texas MD Anderson Cancer Center; University of Washington; Van Andel Research Institute; Vanderbilt University; Washington University; Genome Sequencing Center: Broad Institute; Washington University in St. Louis; Genome Characterization Centers: BC Cancer Agency; Broad Institute; Harvard Medical School; Sidney Kimmel Comprehensive Cancer Center at Johns Hopkins University; University of North Carolina; University of Southern California Epigenome Center; University of Texas MD Anderson Cancer Center; Van Andel Research Institute; Genome Data Analysis Centers: Broad Institute; Brown University:; Harvard Medical School; Institute for Systems Biology; Memorial Sloan Kettering Cancer Center; University of California Santa Cruz; University of Texas MD Anderson Cancer Center; Biospecimen Core Resource: International Genomics Consortium; Research Institute at Nationwide Children's Hospital; Tissue Source Sites: Analytic Biologic Services; Asan Medical Center; Asterand Bioscience; Barretos Cancer Hospital; BioreclamationIVT; Botkin Municipal Clinic; Chonnam National University Medical School; Christiana Care Health System; Cureline; Duke University; Emory University; Erasmus University; Indiana University School of Medicine; Institute of Oncology of Moldova; International Genomics Consortium; Invidumed; Israelitisches Krankenhaus Hamburg; Keimyung University School of Medicine; Memorial Sloan Kettering Cancer Center; National Cancer Center Goyang; Ontario Tumour Bank; Peter MacCallum Cancer Centre; Pusan National University Medical School; Ribeirão Preto Medical School; St. Joseph's Hospital &Medical Center; St. Petersburg Academic University; Tayside Tissue Bank; University of Dundee; University of Kansas Medical Center; University of Michigan; University of North Carolina at Chapel Hill; University of Pittsburgh School of Medicine; University of Texas MD Anderson Cancer Center; Disease Working Group: Duke University; Memorial Sloan Kettering Cancer Center; National Cancer Institute; University of Texas MD Anderson Cancer Center; Yonsei University College of Medicine; Data Coordination Center: CSRA Inc.; Project Team: National Institutes of Health. Integrated genomic characterization of oesophageal carcinoma. Nature 2017;541:169–175.
11. Weaver JM, Ross-Innes CS, Shannon N, Lynch AG, Forshew T, Barbera M, Murtaza M, Ong CA, Lao-Sirieix P, Dunning MJ, Smith L, Smith ML, Anderson CL, Carvalho B, O'Donovan M, Underwood TJ, May AP, Grehan N, Hardwick R, Davies J, Oloumi A, Aparicio S, Caldas C, Eldridge MD, Edwards PA, Rosenfeld N, Tavare S, Fitzgerald RC; OCCAMS Consortium. Ordering of mutations in preinvasive disease stages of esophageal carcinogenesis. Nat Genet 2014;46:837–843.
12. De Silva N, Schulz L, Paterson A, Qain W, Secrier M, Godfrey E, Cheow H, O'Donovan M, Lao-Sirieix P, Jobanputra M, Hochhauser D, Fitzgerald R, Ford H. Molecular effects of lapatinib in the treatment of HER2 overexpressing oesophago-gastric adenocarcinoma. Br J Cancer 2015;113:1305–1312.
13. Secrier M, Li X, de Silva N, Eldridge MD, Contino G, Bornschein J, MacRae S, Grehan N, O'Donovan M, Miremadi A, Yang TP, Bower L, Chettouh H, Crawte J, Galeano-Dalmau N, Grabowska A, Saunders J, Underwood T, Waddell N, Barbour AP, Nutzinger B, Achilleos A, Edwards PA, Lynch AG, Tavare S, Fitzgerald RC; Oesophageal Cancer Clinical and Molecular Stratification (OCCAMS) Consortium. Mutational signatures in esophageal adenocarcinoma define etiologically distinct subgroups with therapeutic relevance. Nat Genet 2016;48:1131–1141.
14. Kim J, Fox C, Peng S, Pusung M, Pectasides E, Matthee E, Hong YS, Do IG, Jang J, Thorner AR, Van Hummelen P, Rustgi AK, Wong KK, Zhou Z, Tang P, Kim KM, Lee J, Bass AJ. Preexisting oncogenic events impact trastuzumab sensitivity in ERBB2-amplified gastroesophageal adenocarcinoma. J Clin Invest 2014; 124:5145–5158.
15. Souza RF. From reflux esophagitis to esophageal adenocarcinoma. Dig Dis 2016;34:483–490.
16. Zhang HY, Zhang Q, Zhang X, Yu C, Huo X, Cheng E, Wang DH, Spechler SJ, Souza RF. Cancer-related inflammation and Barrett's carcinogenesis: interleukin-6 and STAT3 mediate apoptotic resistance in transformed Barrett's cells. Am J Physiol Gastrointest Liver Physiol 2011;300:G454–G460.
17. Dunbar KB, Agoston AT, Odze RD, Huo X, Pham TH, Cipher DJ, Castell DO, Genta RM, Souza RF, Spechler SJ. Association of acute gastroesophageal

reflux disease with esophageal histologic changes. JAMA 2016;315:2104–2112.
18. Duggan SP, Behan FM, Kirca M, Smith S, Reynolds JV, Long A, Kelleher D. An integrative genomic approach in oesophageal cells identifies TRB3 as a bile acid responsive gene, downregulated in Barrett's oesophagus, which regulates NF-kappaB activation and cytokine levels. Carcinogenesis 2010;31:936–945.
19. Duggan SP, Gallagher WM, Fox EJ, Abdel-Latif MM, Reynolds JV, Kelleher D. Low pH induces co-ordinate regulation of gene expression in oesophageal cells. Carcinogenesis 2006;27:319–327.
20. Abdel-Latif MM, O'Riordan J, Windle HJ, Carton E, Ravi N, Kelleher D, Reynolds JV. NF-kappaB activation in esophageal adenocarcinoma: relationship to Barrett's metaplasia, survival, and response to neoadjuvant chemoradiotherapy. Ann Surg 2004;239:491–500.
21. Abdel-Latif MM, O'Riordan JM, Ravi N, Kelleher D, Reynolds JV. Activated nuclear factor-kappa B and cytokine profiles in the esophagus parallel tumor regression following neoadjuvant chemoradiotherapy. Dis Esophagus 2005;18:246–252.
22. Looby E, Abdel-Latif MM, Athie-Morales V, Duggan S, Long A, Kelleher D. Deoxycholate induces COX-2 expression via Erk1/2-, p38-MAPK and AP-1-dependent mechanisms in esophageal cancer cells. BMC Cancer 2009;9:190.
23. Shah SA, Volkov Y, Arfin Q, Abdel-Latif MM, Kelleher D. Ursodeoxycholic acid inhibits interleukin 1 beta [corrected] and deoxycholic acid-induced activation of NF-kappaB and AP-1 in human colon cancer cells. Int J Cancer 2006;118:532–539.
24. Nadatani Y, Huo X, Zhang X, Yu C, Cheng E, Zhang Q, Dunbar KB, Theiss A, Pham TH, Wang DH, Watanabe T, Fujiwara Y, Arakawa T, Spechler SJ, Souza RF. NOD-like receptor protein 3 inflammasome priming and activation in Barrett's epithelial cells. Cell Mol Gastroenterol Hepatol 2016;2:439–453.
25. Duggan SP, Behan FM, Kirca M, Zaheer A, McGarrigle SA, Reynolds JV, Vaz GM, Senge MO, Kelleher D. The characterization of an intestine-like genomic signature maintained during Barrett's-associated adenocarcinogenesis reveals an NR5A2-mediated promotion of cancer cell survival. Sci Rep 2016;6:32638.
26. Wiles AM, Ravi D, Bhavani S, Bishop AJ. An analysis of normalization methods for Drosophila RNAi genomic screens and development of a robust validation scheme. J Biomol Screen 2008;13:777–784.
27. Pelz O, Gilsdorf M, Boutros M. Web cellHTS2: a web-application for the analysis of high-throughput screening data. BMC Bioinformatics 2010;11:185.
28. Rieber N, Knapp B, Eils R, Kaderali L. RNAither, an automated pipeline for the statistical analysis of high-throughput RNAi screens. Bioinformatics 2009;25:678–679.
29. Kim SM, Park YY, Park ES, Cho JY, Izzo JG, Zhang D, Kim SB, Lee JH, Bhutani MS, Swisher SG, Wu X, Coombes KR, Maru D, Wang KK, Buttar NS, Ajani JA, Lee JS. Prognostic biomarkers for esophageal adenocarcinoma identified by analysis of tumor transcriptome. PLoS One 2010;5:e15074.
30. Kimchi ET, Posner MC, Park JO, Darga TE, Kocherginsky M, Karrison T, Hart J, Smith KD, Mezhir JJ, Weichselbaum RR, Khodarev NN. Progression of Barrett's metaplasia to adenocarcinoma is associated with the suppression of the transcriptional programs of epidermal differentiation. Cancer Res 2005;65:3146–3154.
31. Ostrowski J, Mikula M, Karczmarski J, Rubel T, Wyrwicz LS, Bragoszewski P, Gaj P, Dadlez M, Butruk E, Regula J. Molecular defense mechanisms of Barrett's metaplasia estimated by an integrative genomics. J Mol Med 2007;85:733–743.
32. Kilkenny C, Browne WJ, Cuthill IC, Emerson M, Altman DG. Improving bioscience research reporting: the ARRIVE guidelines for reporting animal research. PLoS Biol 2010;8:e1000412.
33. Suljagic M, Longo PG, Bennardo S, Perlas E, Leone G, Laurenti L, Efremov DG. The Syk inhibitor fostamatinib disodium (R788) inhibits tumor growth in the Emu-TCL1 transgenic mouse model of CLL by blocking antigen-dependent B-cell receptor signaling. Blood 2010;116:4894–4905.
34. Zhang JH, Chung TD, Oldenburg KR. A simple statistical parameter for use in evaluation and validation of high throughput screening assays. J Biomol Screen 1999;4:67–73.
35. Su Z, Gay LJ, Strange A, Palles C, Band G, Whiteman DC, Lescai F, Langford C, Nanji M, Edkins S, van der Winkel A, Levine D, Sasieni P, Bellenguez C, Howarth K, Freeman C, Trudgill N, Tucker AT, Pirinen M, Peppelenbosch MP, van der Laan LJW, Kuipers EJ, Drenth JPH, Peters WH, Reynolds JV, Kelleher DP, McManus R, Grabsch H, Prenen H, Bisschops R, Krishnadath K, Siersema PD, van Baal JWPM, Middleton M, Petty R, Gillies R, Burch N, Bhandari P, Paterson S, Edwards C, Penman I, Vaidya K, Ang Y, Murray I, Patel P, Ye W, Mullins P, Wu AH, Bird NC, Dallal H, Shaheen NJ, Murray LJ, Koss K, Bernstein L, Romero Y, Hardie LJ, Zhang R, Winter H, Corley DA, Panter S, Risch HA, Reid BJ, Sargeant I, Gammon MD, Smart H, Dhar A, McMurtry H, Ali H, Liu G, Casson AG, Chow W-H, Rutter M, Tawil A, Morris D, Nwokolo C, Isaacs P, Rodgers C, Ragunath K, MacDonald C, Haigh C, Monk D, Davies G, Wajed S, Johnston D, Gibbons M, Cullen S, Church N, Langley R, Griffin M, Alderson D, Deloukas P, Hunt SE, Gray E, Dronov S, Potter SC, Tashakkori-Ghanbaria A, Anderson M, Brooks C, Blackwell JM, Bramon E, Brown MA, Casas JP, Corvin A, Duncanson A, Markus HS, Mathew CG, Palmer CNA, Plomin R, Rautanen A, Sawcer SJ, Trembath RC, Viswanathan AC, Wood N, Trynka G, Wijmenga C, Cazier J-B, Atherfold P, Nicholson AM, Gellatly NL, Glancy D, Cooper SC, Cunningham D, Lind T, Hapeshi J, Ferry D, Rathbone B, Brown J, Love S, Attwood S, MacGregor S, Watson P, Sanders S, Ek W, Harrison RF, Moayyedi P, de Caestecker J, Barr H, Stupka E, Vaughan TL, Peltonen L, Spencer CCA, Tomlinson I, Donnelly P, Jankowski JAZ. Common variants at the MHC locus and at chromosome 16q24.1 predispose to Barrett's esophagus. Nat Genet 2012;44:1131–1136.

36. Gharahkhani P, Fitzgerald RC, Vaughan TL, Palles C, Gockel I, Tomlinson I, Buas MF, May A, Gerges C, Anders M, Becker J, Kreuser N, Noder T, Venerito M, Veits L, Schmidt T, Manner H, Schmidt C, Hess T, Böhmer AC, Izbicki JR, Hölscher AH, Lang H, Lorenz D, Schumacher B, Hackelsberger A, Mayershofer R, Pech O, Vashist Y, Ott K, Vieth M, Weismüller J, Nöthen MM, Barrett's and Esophageal Adenocarcinoma Consortium (BEACON); Esophageal Adenocarcinoma GenEtics Consortium (EAGLE); Wellcome Trust Case Control Consortium 2 (WTCCC2), Attwood S, Barr H, Chegwidden L, de Caestecker J, Harrison R, Love SB, MacDonald D, Moayyedi P, Prenen H, Watson RGP, Iyer PG, Anderson LA, Bernstein L, Chow WH, Hardie LJ, Lagergren J, Liu G, Risch HA, Wu AH, Ye W, Bird NC, Shaheen NJ, Gammon MD, Corley DA, Caldas C, Moebus S, Knapp M, Peters WHM, Neuhaus H, Rösch T, Ell C, MacGregor S, Pharoah P, Whiteman DC, Jankowski J, Schumacher J. Genome-wide association studies in oesophageal adenocarcinoma and Barrett's oesophagus: a large-scale meta-analysis. Lancet Oncol 2016;17:1363–1373.
37. Bindea G, Mlecnik B, Hackl H, Charoentong P, Tosolini M, Kirilovsky A, Fridman WH, Pages F, Trajanoski Z, Galon J. ClueGO: a Cytoscape plug-in to decipher functionally grouped gene ontology and pathway annotation networks. Bioinformatics 2009;25:1091–1093.
38. Ness-Jensen E, Gottlieb-Vedi E, Wahlin K, Lagergren J. All-cause and cancer-specific mortality in GORD in a population-based cohort study (the HUNT study). Gut 2018;67:209–215.
39. Aran D, Lasry A, Zinger A, Biton M, Pikarsky E, Hellman A, Butte AJ, Ben-Neriah Y. Widespread parainflammation in human cancer. Genome Biol 2016;17:145.
40. Pribluda A, Elyada E, Wiener Z, Hamza H, Goldstein RE, Biton M, Burstain I, Morgenstern Y, Brachya G, Billauer H, Biton S, Snir-Alkalay I, Vucic D, Schlereth K, Mernberger M, Stiewe T, Oren M, Alitalo K, Pikarsky E, Ben-Neriah Y. A senescence-inflammatory switch from cancer-inhibitory to cancer-promoting mechanism. Cancer Cell 2013;24:242–256.
41. van den Berg RH, Faber-Krol MC, Sim RB, Daha MR. The first subcomponent of complement, C1q, triggers the production of IL-8, IL-6, and monocyte chemoattractant peptide-1 by human umbilical vein endothelial cells. J Immunol 1998;161:6924–6930.
42. Faust D, Loos M. In vitro modulation of C1q mRNA expression and secretion by interleukin-1, interleukin-6, and interferon-gamma in resident and stimulated murine peritoneal macrophages. Immunobiology 2002; 206:368–376.
43. Benoit ME, Clarke EV, Morgado P, Fraser DA, Tenner AJ. Complement protein C1q directs macrophage polarization and limits inflammasome activity during the uptake of apoptotic cells. J Immunol 2012;188:5682–5693.
44. Satoh J, Tabunoki H, Ishida T, Yagishita S, Jinnai K, Futamura N, Kobayashi M, Toyoshima I, Yoshioka T, Enomoto K, Arai N, Saito Y, Arima K. Phosphorylated Syk expression is enhanced in Nasu-Hakola disease brains. Neuropathology 2012;32:149–157.
45. Paradowska-Gorycka A, Jurkowska M. Structure, expression pattern and biological activity of molecular complex TREM-2/DAP12. Hum Immunol 2013; 74:730–737.
46. Chauhan AK, Moore TL. Immune complexes and late complement proteins trigger activation of Syk tyrosine kinase in human CD4(+) T cells. Clin Exp Immunol 2012; 167:235–245.
47. Szasz AM, Lanczky A, Nagy A, Forster S, Hark K, Green JE, Boussioutas A, Busuttil R, Szabo A, Gyorffy B. Cross-validation of survival associated biomarkers in gastric cancer using transcriptomic data of 1,065 patients. Oncotarget 2016;7:49322–49333.
48. Quante M, Bhagat G, Abrams JA, Marache F, Good P, Lee MD, Lee Y, Friedman R, Asfaha S, Dubeykovskaya Z, Mahmood U, Figueiredo JL, Kitajewski J, Shawber C, Lightdale CJ, Rustgi AK, Wang TC. Bile acid and inflammation activate gastric cardia stem cells in a mouse model of Barrett-like metaplasia. Cancer Cell 2012;21:36–51.
49. Piccio L, Buonsanti C, Cella M, Tassi I, Schmidt RE, Fenoglio C, Rinker J 2nd, Naismith RT, Panina-Bordignon P, Passini N, Galimberti D, Scarpini E, Colonna M, Cross AH. Identification of soluble TREM-2 in the cerebrospinal fluid and its association with multiple sclerosis and CNS inflammation. Brain 2008; 131:3081–3091.
50. Chen G, Tan CS, Teh BK, Lu J. Molecular mechanisms for synchronized transcription of three complement C1q subunit genes in dendritic cells and macrophages. J Biol Chem 2011;286:34941–34950.
51. Wagner RT, Xu X, Yi F, Merrill BJ, Cooney AJ. Canonical Wnt/beta-catenin regulation of liver receptor homolog-1 mediates pluripotency gene expression. Stem Cells 2010;28:1794–1804.
52. Naito AT, Sumida T, Nomura S, Liu ML, Higo T, Nakagawa A, Okada K, Sakai T, Hashimoto A, Hara Y, Shimizu I, Zhu W, Toko H, Katada A, Akazawa H, Oka T, Lee JK, Minamino T, Nagai T, Walsh K, Kikuchi A, Matsumoto M, Botto M, Shiojima I, Komuro I. Complement C1q activates canonical Wnt signaling and promotes aging-related phenotypes. Cell 2012; 149:1298–1313.
53. Okada K, Naito AT, Higo T, Nakagawa A, Shibamoto M, Sakai T, Hashimoto A, Kuramoto Y, Sumida T, Nomura S, Ito M, Yamaguchi T, Oka T, Akazawa H, Lee JK, Morimoto S, Sakata Y, Shiojima I, Komuro I. Wnt/beta-catenin signaling contributes to skeletal myopathy in heart failure via direct interaction with forkhead box O. Circ Heart Fail 2015;8:799–808.
54. Jiang T, Yu JT, Zhu XC, Tan MS, Gu LZ, Zhang YD, Tan L. Triggering receptor expressed on myeloid cells 2 knockdown exacerbates aging-related neuroinflammation and cognitive deficiency in senescence-accelerated mouse prone 8 mice. Neurobiol Aging 2014;35:1243–1251.
55. Jonsson T, Stefansson H, Steinberg S, Jonsdottir I, Jonsson PV, Snaedal J, Bjornsson S, Huttenlocher J, Levey AI, Lah JJ, Rujescu D, Hampel H, Giegling I, Andreassen OA, Engedal K, Ulstein I, Djurovic S,

Ibrahim-Verbaas C, Hofman A, Ikram MA, van Duijn CM, Thorsteinsdottir U, Kong A, Stefansson K. Variant of TREM2 associated with the risk of Alzheimer's disease. N Engl J Med 2013;368:107–116.

56. Kobayashi M, Konishi H, Sayo A, Takai T, Kiyama H. TREM2/DAP12 signal elicits proinflammatory response in microglia and exacerbates neuropathic pain. J Neurosci 2016;36:11138–11150.
57. Weinblatt ME, Kavanaugh A, Burgos-Vargas R, Dikranian AH, Medrano-Ramirez G, Morales-Torres JL, Murphy FT, Musser TK, Straniero N, Vicente-Gonzales AV, Grossbard E. Treatment of rheumatoid arthritis with a Syk kinase inhibitor: a twelve-week, randomized, placebo-controlled trial. Arthritis Rheum 2008; 58:3309–3318.
58. Weinblatt ME, Kavanaugh A, Genovese MC, Musser TK, Grossbard EB, Magilavy DB. An oral spleen tyrosine kinase (Syk) inhibitor for rheumatoid arthritis. N Engl J Med 2010;363:1303–1312.
59. Flinn IW, Bartlett NL, Blum KA, Ardeshna KM, LaCasce AS, Flowers CR, Shustov AR, Thress KS, Mitchell P, Zheng F, Skolnik JM, Friedberg JW. A phase II trial to evaluate the efficacy of fostamatinib in patients with relapsed or refractory diffuse large B-cell lymphoma (DLBCL). Eur J Cancer 2016;54:11–17.
60. Smith J, McDaid JP, Bhangal G, Chawanasuntorapoj R, Masuda ES, Cook HT, Pusey CD, Tam FW. A spleen tyrosine kinase inhibitor reduces the severity of established glomerulonephritis. J Am Soc Nephrol 2010; 21:231–236.
61. Rolf MG, Curwen JO, Veldman-Jones M, Eberlein C, Wang J, Harmer A, Hellawell CJ, Braddock M. In vitro pharmacological profiling of R406 identifies molecular targets underlying the clinical effects of fostamatinib. Pharmacol Res Perspect 2015;3:e00175.
62. Lasry A, Aran D, Butte AJ, Ben-Neriah Y. Cancer cell-autonomous parainflammation mimics immune cell infiltration. Cancer Res 2017;77:3740–3744.
63. Patel AP, Tirosh I, Trombetta JJ, Shalek AK, Gillespie SM, Wakimoto H, Cahill DP, Nahed BV, Curry WT, Martuza RL, Louis DN, Rozenblatt-Rosen O, Suva ML, Regev A, Bernstein BE. Single-cell RNA-seq highlights intratumoral heterogeneity in primary glioblastoma. Science 2014;344:1396–1401.
64. Lu R, Pal J, Buon L, Nanjappa P, Shi J, Fulciniti M, Tai YT, Guo L, Yu M, Gryaznov S, Munshi NC, Shammas MA. Targeting homologous recombination and telomerase in Barrett's adenocarcinoma: impact on telomere maintenance, genomic instability and tumor growth. Oncogene 2014;33:1495–1505.
65. Pal J, Bertheau R, Buon L, Qazi A, Batchu RB, Bandyopadhyay S, Ali-Fehmi R, Beer DG, Weaver DW, Shmookler Reis RJ, Goyal RK, Huang Q, Munshi NC, Shammas MA. Genomic evolution in Barrett's adenocarcinoma cells: critical roles of elevated hsRAD51, homologous recombination and Alu sequences in the genome. Oncogene 2011;30:3585–3598.
66. Pal J, Fulciniti M, Nanjappa P, Buon L, Tai YT, Tassone P, Munshi NC, Shammas MA. Targeting PI3K and RAD51 in Barrett's adenocarcinoma: impact on DNA damage checkpoints, expression profile and tumor growth. Cancer Genomics Proteomics 2012;9:55–66.
67. Palles C, Chegwidden L, Li X, Findlay JM, Farnham G, Castro Giner F, Peppelenbosch MP, Kovac M, Adams CL, Prenen H, Briggs S, Harrison R, Sanders S, MacDonald D, Haigh C, Tucker A, Love S, Nanji M, deCaestecker J, Ferry D, Rathbone B, Hapeshi J, Barr H, Moayyedi P, Watson P, Zietek B, Maroo N, Gay L, Underwood T, Boulter L, McMurtry H, Monk D, Patel P, Ragunath K, Al Dulaimi D, Murray I, Koss K, Veitch A, Trudgill N, Nwokolo C, Rembacken B, Atherfold P, Green E, Ang Y, Kuipers EJ, Chow W, Paterson S, Kadri S, Beales I, Grimley C, Mullins P, Beckett C, Farrant M, Dixon A, Kelly S, Johnson M, Wajed S, Dhar A, Sawyer E, Roylance R, Onstad L, Gammon MD, Corley DA, Shaheen NJ, Bird NC, Hardie LJ, Reid BJ, Ye W, Liu G, Romero Y, Bernstein L, Wu AH, Casson AG, Fitzgerald R, Whiteman DC, Risch HA, Levine DM, Vaughan TL, Verhaar AP, van den Brande J, Toxopeus EL, Spaander MC, Wijnhoven BP, van der Laan LJ, Krishnadath K, Wijmenga C, Trynka G, McManus R, Reynolds JV, O'Sullivan J, MacMathuna P, McGarrigle SA, Kelleher D, Vermeire S, Cleynen I, Bisschops R, Tomlinson I, Jankowski J. Polymorphisms near TBX5 and GDF7 are associated with increased risk for Barrett's esophagus. Gastroenterology 2015; 148:367–378.
68. Cunningham D, Stenning SP, Smyth EC, Okines AF, Allum WH, Rowley S, Stevenson L, Grabsch HI, Alderson D, Crosby T, Griffin SM, Mansoor W, Coxon FY, Falk SJ, Darby S, Sumpter KA, Blazeby JM, Langley RE. Peri-operative chemotherapy with or without bevacizumab in operable oesophagogastric adenocarcinoma (UK Medical Research Council ST03): primary analysis results of a multicentre, open-label, randomised phase 2-3 trial. Lancet Oncol 2017;18:357–370.
69. Alonso R, Salavert F, Garcia-Garcia F, Carbonell-Caballero J, Bleda M, Garcia-Alonso L, Sanchis-Juan A, Perez-Gil D, Marin-Garcia P, Sanchez R, Cubuk C, Hidalgo MR, Amadoz A, Hernansaiz-Ballesteros RD, Aleman A, Tarraga J, Montaner D, Medina I, Dopazo J. Babelomics 5.0: functional interpretation for new generations of genomic data. Nucleic Acids Res 2015; 43:W117–W121.
70. Medina I, Carbonell J, Pulido L, Madeira SC, Goetz S, Conesa A, Tarraga J, Pascual-Montano A, Nogales-Cadenas R, Santoyo J, Garcia F, Marba M, Montaner D, Dopazo J. Babelomics: an integrative platform for the analysis of transcriptomics, proteomics and genomic data with advanced functional profiling. Nucleic Acids Res 2010;38:W210–W213.
71. Roumenina LT, Sene D, Radanova M, Blouin J, Halbwachs-Mecarelli L, Dragon-Durey MA, Fridman WH, Fremeaux-Bacchi V. Functional complement C1q abnormality leads to impaired immune complexes and apoptotic cell clearance. J Immunol 2011;187:4369–4373.
72. Kim BC, Hwang HJ, An HT, Lee H, Park JS, Hong J, Ko J, Kim C, Lee JS, Ko YG. Antibody neutralization of cell-surface gC1qR/HABP1/SF2-p32 prevents lamellipodia formation and tumorigenesis. Oncotarget 2016; 7:49972–49985.

73. Kim KB, Yi JS, Nguyen N, Lee JH, Kwon YC, Ahn BY, Cho H, Kim YK, Yoo HJ, Lee JS, Ko YG. Cell-surface receptor for complement component C1q (gC1qR) is a key regulator for lamellipodia formation and cancer metastasis. J Biol Chem 2011;286:23093–23101.
74. Colonna M, Wang Y. TREM2 variants: new keys to decipher Alzheimer disease pathogenesis. Nat Rev Neurosci 2016;17:201–207.
75. Forabosco P, Ramasamy A, Trabzuni D, Walker R, Smith C, Bras J, Levine AP, Hardy J, Pocock JM, Guerreiro R, Weale ME, Ryten M. Insights into TREM2 biology by network analysis of human brain gene expression data. Neurobiol Aging 2013;34:2699–2714.
76. Heslegrave A, Heywood W, Paterson R, Magdalinou N, Svensson J, Johansson P, Ohrfelt A, Blennow K, Hardy J, Schott J, Mills K, Zetterberg H. Increased cerebrospinal fluid soluble TREM2 concentration in Alzheimer's disease. Mol Neurodegener 2016;11:3.
77. Walter J. The triggering receptor expressed on myeloid cells 2: a molecular link of neuroinflammation and neurodegenerative diseases. J Biol Chem 2016;291:4334–4341.
78. Hong S, Beja-Glasser VF, Nfonoyim BM, Frouin A, Li S, Ramakrishnan S, Merry KM, Shi Q, Rosenthal A, Barres BA, Lemere CA, Selkoe DJ, Stevens B. Complement and microglia mediate early synapse loss in Alzheimer mouse models. Science 2016;352:712–716.
79. Stevens B, Allen NJ, Vazquez LE, Howell GR, Christopherson KS, Nouri N, Micheva KD, Mehalow AK, Huberman AD, Stafford B, Sher A, Litke AM, Lambris JD, Smith SJ, John SW, Barres BA. The classical complement cascade mediates CNS synapse elimination. Cell 2007;131:1164–1178.
80. Wang XQ, Tao BB, Li B, Wang XH, Zhang WC, Wan L, Hua XM, Li ST. Overexpression of TREM2 enhances glioma cell proliferation and invasion: a therapeutic target in human glioma. Oncotarget 2016;7:2354–2366.
81. Gyorffy B, Surowiak P, Budczies J, Lanczky A. Online survival analysis software to assess the prognostic value of biomarkers using transcriptomic data in non-small-cell lung cancer. PLoS One 2013;8:e82241.
82. Kunwar S, Devkota AR, Ghimire DK. Fostamatinib, an oral spleen tyrosine kinase inhibitor, in the treatment of rheumatoid arthritis: a meta-analysis of randomized controlled trials. Rheumatol Int 2016;36:1077–1087.
83. McAdoo SP, Reynolds J, Bhangal G, Smith J, McDaid JP, Tanna A, Jackson WD, Masuda ES, Cook HT, Pusey CD, Tam FW. Spleen tyrosine kinase inhibition attenuates autoantibody production and reverses experimental autoimmune GN. J Am Soc Nephrol 2014;25:2291–2302.
84. Raz R, Lee CK, Cannizzaro LA, d'Eustachio P, Levy DE. Essential role of STAT3 for embryonic stem cell pluripotency. Proc Natl Acad Sci U S A 1999;96:2846–2851.
85. Tang Y, Luo Y, Jiang Z, Ma Y, Lin CJ, Kim C, Carter MG, Amano T, Park J, Kish S, Tian XC. Jak/Stat3 signaling promotes somatic cell reprogramming by epigenetic regulation. Stem Cells 2012;30:2645–2656.

Received August 24, 2017. Accepted January 12, 2018.

Correspondence
Address correspondence to: Shane P. Duggan, Rm 5.408 Life Sciences Institute, Health Sciences Mall, University of British Columbia, Vancouver, BC Canada V6T 1Z3. e-mail: shane.duggan@ubc.ca or Dermot Kelleher, 317 - 2194 Health Sciences Mall, Vancouver, BC Canada V6T 1Z3. e-mail: dermot.kelleher@ubc.ca.

Acknowledgments
The authors thank Anthony Davies, Rocio Seoane, and Lucy Baudino for technical support.

Author contributions
S. P. Duggan and C. Garry performed and designed the studies; F. M. Behan and S. Phipps contributed to technical components of screening implementation; A. Zaheer, M. Kirca, J. V. Reynolds, S. McGarrigle, H. Kudo, R. Goldin, S. E. Kalloger, and D. F. Schaeffer provided clinical and pathologic support and analyses; S. P. Duggan and J. Strid performed and evaluated animal model experiments; A. Long provided in vitro experimental expertise and interpretation; S. P. Duggan and D. Kelleher planned the study design and supervised the study; and all authors edited the manuscript.

Conflicts of interest
The authors disclose no conflicts.

Funding
Supported by the Health Research Board Ireland (HRB-TRA.2007.11 (S.D., C.G., S.P., D.K., A.L.) and the HRB PhD Scholars program (F.M.B.)), Imperial College London (H.K., R.G., J.S., D.K.), the University of British Columbia Start-up funds F15-04616, and a donation in memoriam by the Chan family (S.D., D.K.).